Second-harmonic-generation spectra of the hexagonal manganites $RMnO_3$

2001 J. Phys.: Condens. Matter 13 3031

(http://iopscience.iop.org/0953-8984/13/13/316)

INSTITUTE OF PHYSICS PUBLISHING JOURNAL OF PHYSICS: CONDENSED MATTER

J. Phys.: Condens. Matter **13** (2001) 3031–3055 www.iop.org/Journals/cm PII: S0953-8984(01)19896-6

Second-harmonic-generation spectra of the hexagonal manganites $RMnO_3$

Takako Iizuka-Sakano[1], **Eiichi Hanamura**[2] **and Yukito Tanabe**[3]

[1] Electrotechnical Laboratory, 1-1-4 Umezono, Tsukuba, Ibaraki 305-8568, Japan
[2] Chitose Institute of Science and Technology and CREST, JST (Japan Science and Technology Corporation), 785-65 Bibi, Chitose-City, Hokkaido 066-8655, Japan
[3] Department of Applied Physics, University of Tokyo, 7-3-1 Hongo, Bunkyo-ku, Tokyo 113-8656, Japan

Received 8 December 2000

Abstract

Non-linear susceptibilities for use in describing the second-harmonic generation (SHG) recently observed in the hexagonal manganites $RMnO_3$ (R = Sc, Y, Ho, Er, Tm, Yb, Lu) below the Néel temperature T_N are derived. Their explicit expressions show that they should give rise to quite different spectra according to whether the magnetic ordering is $P6_3'cm'$ or $P6_3'c'm$. The excited states around 2.45 eV are treated as excitons in the antiferromagnetic phase. The calculated SHG spectra are compared with experiments and it is found that they can be used to explain the observed features and spectra satisfactorily.

1. Introduction

Optical second-harmonic spectroscopy has proved to be a powerful means of determination of complex magnetic structures—for example, the non-collinear antiferromagnetic structure of the hexagonal manganites $RMnO_3$ (R = Sc, Y, Ho, Er, Tm, Yb, Lu) [1–3].

These compounds are paraelectric above T_C (between 550 and 1000 K) with the space group $P6_3/mmc$ and ferroelectric below T_C with the space group $P6_3cm$. They are antiferromagnetic below T_N which is around 80 K.

We take the case of $YMnO_3$ as our first example. Below $T_N = 73.49$ K, second-harmonic generation (SHG) is observed in the region around 2.45 eV; it corresponds to the magnetic non-linear susceptibility $\chi^{(c)}_{yyy}$. This corresponds to the magnetic space group $P6_3'cm'$ and we know that the spin ordering should be as shown in the left-hand part of figure 1 of reference [3], i.e., α_1-type with the angle $\varphi = 0$. The susceptibility here is the yyy-component of a time-non-invariant tensor (c-tensor) as indicated by the superscript (c), with the xy-axes given in the figure referred to above. The two peaks in the SHG spectra around 2.45 eV seem to indicate the existence of two excited levels at that energy and constructive interference between the susceptibilities associated with each level (figure 1(b) of reference [1]).

On the other hand, in $ErMnO_3$, SHG below $T_N = 78.64$ K at around 2.45 eV is observed only in the configuration corresponding to the non-vanishing susceptibility $\chi^{(c)}_{xxx}$. This means that the magnetic space group for this system is $P6_3'c'm$ and the spins of the Mn ions are all rotated by an angle of 90° compared to those of $YMnO_3$—that is, the ordering is of α_2-type. There are two peaks also in this case, but with destructive interference with a dip between them [1].

The spectra of $HoMnO_3$ ($T_N = 74.87$ K) are interesting in that they can show either of the behaviours described above depending on the temperature. The peaks at 2.45 eV show constructive interference for $\chi^{(c)}_{yyy}$ below $T_R = 42$ K and destructive interference for $\chi^{(c)}_{xxx}$ above T_R due to the rotation of the spins by 90° in the xy-plane [3].

The observation of the time-invariant $\chi^{(i)}_{zxx}$ related to the ferroelectricity gives the position of an excited level at 2.7 eV for all of these systems [2].

The purpose of the present paper is to try to explain these features of the SHG spectra as well as to clarify the relations between them and the magnetic structures of the hexagonal manganites through the calculation of the susceptibilities $\chi^{(c)}_{yyy}$ and $\chi^{(c)}_{xxx}$, which are simply denoted as χ_{yyy} and χ_{xxx} in the present paper. In the next section we describe the crystal magnetic symmetry of the present system. The environment of the Mn ions to be treated here is unusual in that Mn^{3+} ions with total spin $S = 2$ are surrounded by fivefold-coordinated (trigonal) bipyramids of O^{2-} ions. The electronic states involved will be discussed in section 3. There are six Mn sites in a unit cell of the antiferromagnetic phase. In section 4, we describe how to correlate wave functions at six different sites. Section 5 is the core of the present paper. We find here that the single-ion theory does not work well, and develop the exciton theory for the excited states around 2.45 eV. The susceptibilities obtained in the exciton mode turn out to be satisfactory. They predict two excited levels near the single level expected in the single-ion theory and quite different interference behaviours for χ_{yyy} and χ_{xxx}. In section 6.1, we give a brief discussion of possible causes of clamping of the two order parameters, ferroelectric and antiferromagnetic. A comparison of the calculated spectra with the observed ones is made in section 6.2. The final section is devoted to a discussion and conclusions. In the appendix, the mechanism of exciton transfer treated in section 5.2 is described, so that the physical meanings of the parameters which appeared in the exciton theory are made clear.

2. Crystal and magnetic structure of $RMnO_3$

The crystal structure of ferroelectric $RMnO_3$ (R = Y, Ho, Er, Lu) is reported by Yakel *et al* [4]. The x- and y-axes chosen in the present paper coincide with theirs and those of reference [3] as well.

There are six Mn ions in a magnetic unit cell. Their sites in the unit cell and our choice of local axis ξ_i and η_i are shown in figure 1, where the local ξ_1- and η_1-axes at site 1 are chosen parallel to the global x- and y-axes.

As seen in the figure, three Mn_i ions ($i = 1, 2, 3$) are assumed to lie on the $z = 0$ plane, while the other three with $i = 4, 5, 6$ are on the $z = c/2$ plane, where c is the height of the unit cell. Let us further assume that the coordinate of Mn_1 is given by $(d, 0, 0)$ with $d \sim 0.3a$ and that of Mn_4 by $(-d, 0, c/2)$ in terms of the lattice constant a, so that either $\sigma_d(\boldsymbol{\tau})$ or $\theta\sigma_d(\boldsymbol{\tau})$ carries Mn_1 into Mn_4 with its environment in the crystal, where $\sigma_d(\boldsymbol{\tau})$ is the reflection in the yz-plane followed by the translation $\boldsymbol{\tau} = (0, 0, c/2)$ and θ is the time reversal.

Suppose the local ξ_i- and η_i-axes are obtained by rotating the global x- and y-axes by an angle ϑ_i. We then have the following relations:

$$P_x = P_{\xi_i} \cos\vartheta_i - P_{\eta_i} \sin\vartheta_i \tag{1}$$

$$P_y = P_{\xi_i} \sin\vartheta_i + P_{\eta_i} \cos\vartheta_i \tag{2}$$

between the components of electric dipole-moment operators at different sites, which will be used in section 5.1.

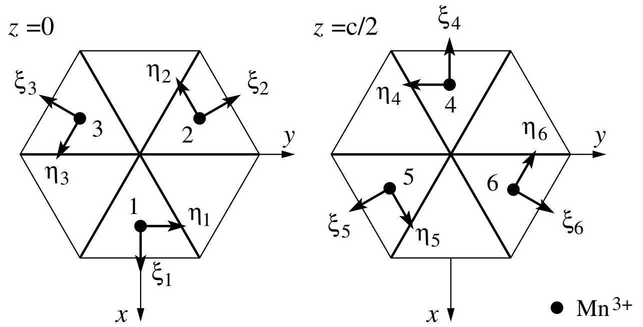

Figure 1. Six Mn sites in the unit cell and the local coordinate axes.

To avoid confusion, we follow Fiebig *et al* [3] in the choice of symmetry operations of the two possible magnetic space groups (a) $P6_3'cm'$ (spins of $Mn_1 \parallel \boldsymbol{x}$) and (b) $P6_3'c'm$ (spins of $Mn_1 \parallel \boldsymbol{y}$). They are given by

$$\text{(a) } P6_3'cm'\colon \begin{aligned} 6_3' &= \theta C_6(\boldsymbol{\tau}) \\ c &= \sigma_d(\boldsymbol{\tau}) \\ m' &= \theta\sigma_v \end{aligned} \tag{3}$$

$$\text{(b) } P6_3'c'm\colon \begin{aligned} 6_3' &= \theta C_6(\boldsymbol{\tau}) \\ c' &= \theta\sigma_d(\boldsymbol{\tau}) \\ m &= \sigma_v \end{aligned} \tag{4}$$

where σ_v is the reflection in the xz-plane. It must be mentioned that the intermediate symmetry $P6_3'$ is possible, as found in $ScMnO_3$, where we have the spins of Mn_1 making any angle φ with the reference axis [5].

For the spin ordering corresponding to these magnetic space groups, the reader is referred to figure 1 of reference [3]. Although we have mentioned in the above that the spins of Mn_1 are parallel to $\boldsymbol{x}$ in $P6_3'cm'$, this is not quite correct. They may also have z-components, i.e., they can cant out of the xy-plane without lowering the symmetry described by this group. In contrast to this, the spins of Mn_1 have to be parallel to $\boldsymbol{y}$ in $P6_3'c'm$.

3. Electronic states of a Mn^{3+} ion in $RMnO_3$

Let us first consider the electronic states of a Mn_1 ion in the paraelectric phase described by $P6_3/mmc$ [6]. The Mn_1 in this phase is located at the centre of a fivefold-coordinated (trigonal) bipyramid of O^{2-} ions with $D_{3h} = \bar{6}m2$ symmetry with the twofold-symmetry axis of the bipyramid chosen as the x-axis [4, 7].

As the energy level scheme for the four localized d electrons with their spins parallel ($S = 2$) in this unusual fivefold coordination, we adopt the one proposed by reference [1]. In this model, the ground state is the orbital singlet ${}^5A_1 \equiv {}^5\Gamma_1$. The first and second (quintet) excited states are ${}^5E_2 \equiv {}^5\Gamma_5$ and ${}^5E_1 \equiv {}^5\Gamma_6$, respectively.

The wave functions corresponding to these levels are given by

$$\Phi(E_1a) = \Phi_{zx} \tag{5}$$

$$\Phi(E_1b) = \Phi_{zy} \tag{6}$$

$$\Phi(E_2a) = c\Phi_{x^2-y^2} + c'\Phi_x \tag{7}$$

$$\Phi(\mathrm{E_2b}) = c\Phi_{-2xy} + c'\Phi_y \tag{8}$$

$$\Phi(\mathrm{A_1}) = \Phi_{z^2} \tag{9}$$

with $c^2 + c'^2 = 1$, where we have specified only the symmetry labels for the orbital states. The spin quantum numbers M_x or M_y are not given explicitly. For degenerate representations, the two substates of $\mathrm{E_1}$, for example, are denoted as $\mathrm{E_1a}$ and $\mathrm{E_1b}$. The functions on the right-hand side of these equations are given by

$$\Phi_{zx} = \frac{1}{\sqrt{2}}(-\Phi(D, +1) + \Phi(D, -1)) \tag{10}$$

$$\Phi_{zy} = \frac{\mathrm{i}}{\sqrt{2}}(\Phi(D, +1) + \Phi(D, -1)) \tag{11}$$

$$\Phi_{x^2-y^2} = \frac{1}{\sqrt{2}}(\Phi(D, +2) + \Phi(D, -2)) \tag{12}$$

$$\Phi_{-2xy} = \frac{\mathrm{i}}{\sqrt{2}}(\Phi(D, +2) - \Phi(D, -2)) \tag{13}$$

$$\Phi_{z^2} = \Phi(D, 0) \tag{14}$$

in terms of $\mathrm{d^4\ ^5D}$ wave functions. Note that (Φ_x, Φ_y) in equations (7) and (8) are the states with odd parity, transforming like (x, y) under $\mathrm{D_{3h}}$. The presence of these states on the right-hand side of these equations is, of course, due to the lack of the inversion symmetry in the present system. We assume the coefficient c' to be small but not negligible compared with c. In other words, we expect appreciable d–p mixing for the present system. It makes direct electric dipole transitions from $\Phi(\mathrm{A_1})$ to $\Phi(\mathrm{E_2a})$ and $\Phi(\mathrm{E_2b})$ possible and the transitions are associated with the strong absorption in $\mathrm{YMnO_3}$ above 1.55 eV [1].

In the ferroelectric phase, the Mn ion is surrounded by a distorted (and tilted) bipyramid of $\mathrm{O^{2-}}$ ions, the site symmetry being $\mathrm{C_s} = m = \{E, \sigma_v\}$, where $\sigma_v = \sigma_y$, the reflection in the xz-plane. The effect of this distortion will be treated as a perturbation due to fields having symmetry lower than $\mathrm{D_{3h}}$. Naturally, the compatibility between $\mathrm{D_{3h}}$ and $\mathrm{C_s}$ (resulting from the descent in symmetry) restricts the symmetry of the perturbing field V_m as follows:

$$V_m = V(\mathrm{B_2}) + V(\mathrm{E_1a}) + V(\mathrm{E_2a}) \tag{15}$$

where $V(\Gamma) = \sum_i v_i(\Gamma)$. Let us give, for simplicity, only terms of lowest orders for the low-symmetry fields: $v_i(\mathrm{B_2}) = Az_i$, $v_i(\mathrm{E_1a}) = Bz_ix_i$, and $v_i(\mathrm{E_2a}) = Cx_i + D(x_i^2 - y_i^2)$ in terms of the coordinates (x_i, y_i, z_i) for the ith electron.

The field $V(\mathrm{E_2a})$ lifts the twofold degeneracy of the $\mathrm{E_1}$ as well as that of $\mathrm{E_2}$ states of $\mathrm{D_{3h}}$, whereas $V(\mathrm{B_2})$ and $V(\mathrm{E_1a})$ bring in the mixing among the unperturbed states:

$$\Psi_1 = \Phi(\mathrm{E_1a}) + \Phi(\mathrm{E_2a})\langle \mathrm{E_2a}|V_m|\mathrm{E_1a}\rangle/\Delta E(1, 3) \tag{16}$$

$$\Psi_2 = \Phi(\mathrm{E_1b}) + \Phi(\mathrm{E_2b})\langle \mathrm{E_2b}|V_m|\mathrm{E_1b}\rangle/\Delta E(2, 4) \tag{17}$$

$$\Psi_3 = \Phi(\mathrm{E_2a}) - \Phi(\mathrm{E_1a})\langle \mathrm{E_1a}|V_m|\mathrm{E_2a}\rangle/\Delta E(1, 3) \tag{18}$$

$$\Psi_4 = \Phi(\mathrm{E_2b}) - \Phi(\mathrm{E_1b})\langle \mathrm{E_1b}|V_m|\mathrm{E_2b}\rangle/\Delta E(2, 4) \tag{19}$$

$$\Psi_0 = \Phi(\mathrm{A_1}) - \Phi_z\langle \Phi_z|V_m|\mathrm{A_1}\rangle/\Delta E_z \tag{20}$$

where $\Psi_{1,3}$ are even under σ_v (Γ_1 of $\mathrm{C_s}$ in Bethe's notation), while $\Psi_{2,4}$ are odd (Γ_2). The energy of the state Ψ_i will be denoted as E_i in the following with $\Delta E(i, j) = E_i - E_j$. The wave function Φ_z transforming like z represents an odd-parity state, with its excitation energy ΔE_z.

Unlike in figure 2 of reference [1], in this paper the highest level is assigned to the state $^5E_1a \equiv {}^5\Gamma_1$ with its energy E_1, because the corresponding peak at 2.7 eV is observed in χ_{zxx}-spectra of $YMnO_3$. This then implies that our $^5E_1b \equiv {}^5\Gamma_2$ with its energy E_2 is to be associated with the peak at 2.45 eV of the χ_{yyy}-spectra.

Let us consider the spin–orbit interaction

$$\mathcal{H}_{so} = \lambda \boldsymbol{S} \cdot \boldsymbol{L} \tag{21}$$

as the next perturbation, where λ is related to the parameter ζ for a single electron as $\lambda = \zeta/4$.

The matrix of the spin–orbit interaction is given by

$$\begin{array}{cc} & \begin{array}{ccccc} \Phi(A_1) & \Phi(E_1a) & \Phi(E_1b) & \Phi(E_2a) & \Phi(E_2b) \end{array} \\ \begin{array}{c} \Phi(A_1) \\ \Phi(E_1a) \\ \Phi(E_1b) \\ \Phi(E_2a) \\ \Phi(E_2b) \end{array} & \begin{pmatrix} 0 & -i\sqrt{3}\lambda S_y & i\sqrt{3}\lambda S_x & 0 & 0 \\ i\sqrt{3}\lambda S_y & 0 & -i\lambda S_z & -i\lambda c S_y & -i\lambda c S_x \\ -i\sqrt{3}\lambda S_x & i\lambda S_z & 0 & -i\lambda c S_x & i\lambda c S_y \\ 0 & i\lambda c S_y & i\lambda c S_x & 0 & 2i\lambda c^2 S_z \\ 0 & i\lambda c S_x & -i\lambda c S_y & -2i\lambda c^2 S_z & 0 \end{pmatrix} \end{array}. \tag{22}$$

Note that we are not specifying the direction of the spin yet, so the spin components involved are left simply as operators within the spin space. The spin–orbit interaction introduces further mixing among the unperturbed states which makes spin-dependent transitions possible in section 5.

4. Choice of wave functions at different sites

Wave functions $\psi_\lambda(\alpha)$ ($\psi_\lambda \equiv \Psi_\lambda$, including spin) at different sites α are related to each other by the following relations:

$$C_3\psi_\lambda(1) = \psi_\lambda(2) \qquad C_3^{-1}\psi_\lambda(1) = \psi_\lambda(3) \tag{23}$$

$$C_3\psi_\lambda(4) = \psi_\lambda(5) \qquad C_3^{-1}\psi_\lambda(4) = \psi_\lambda(6). \tag{24}$$

We further have, in case (a),

$$\sigma_d(\boldsymbol{\tau})\psi_1(1) = \psi_1(4) \tag{25}$$

$$\sigma_d(\boldsymbol{\tau})\psi_2(1) = -\psi_2(4) \tag{26}$$

and, in case (b),

$$\theta\sigma_d(\boldsymbol{\tau})\psi_1(1) = \psi_1(4) \tag{27}$$

$$\theta\sigma_d(\boldsymbol{\tau})\psi_2(1) = -\psi_2(4). \tag{28}$$

Note that the λ-indices 1 and 2 refer to the two components E_1a and E_1b of the doublet $^5E_1$, respectively, and that the orbital part of $\psi_1(1)$ is even, while that of $\psi_2(1)$ is odd under σ_v.

5. Calculation of non-linear susceptibilities

Let us first write down the expressions for the non-linear susceptibilities involved in the present problem [8–10], before proceeding to the details of the calculation.

The expression for the susceptibility may be given as

$$\chi_{\alpha\beta\gamma} = \frac{1}{\epsilon_0\hbar^2}\sum_i \rho_i \left[\sum_{m,k}\frac{(P\ P\ P)_{imki}}{(\omega_{mi}-2\omega)(\omega_{ki}-\omega)} + \sum_{m,m'}\frac{(P\ P\ P)_{imm'i}}{(\omega_{mi}+\omega)(\omega_{m'i}-\omega)} \right.$$
$$\left. + \sum_{m,k}\frac{(P\ P\ P)_{ikmi}}{(\omega_{mi}+2\omega)(\omega_{ki}+\omega)}\right] \tag{29}$$

with ω_{mi} denoting the energy difference between the states $|m\rangle$ and $|i\rangle$, ρ_i the thermal distribution of the initial state $|i\rangle$, and

$$\begin{aligned}(P\ P\ P)_{imki} &= (P_\alpha)_{im}(P_\beta)_{mk}(P_\gamma)_{ki}\\ (P\ P\ P)_{imm'i} &= (P_\alpha)_{im}(P_\beta)_{mm'}(P_\gamma)_{m'i}\\ (P\ P\ P)_{ikmi} &= (P_\alpha)_{ik}(P_\beta)_{km}(P_\gamma)_{mi}.\end{aligned} \tag{30}$$

The dominant term corresponding to the two-photon resonance is given by

$$\chi_{\alpha\beta\gamma} = \frac{1}{\epsilon_0}\sum_i \rho_i \sum_m \frac{(P_\alpha)_{im}(P_\beta P_\gamma)_{mi}}{(\Delta E_{mi} - 2\hbar\omega)\,\Delta E} \tag{31}$$

with the closure approximation [9], where $\Delta E_{mi} = \hbar\omega_{mi}$ and $1/\Delta E$ stands for a certain average of $1/(\Delta E(k,i) - \hbar\omega)$ over odd-parity states $|k\rangle$.

If we choose P and the states $|m\rangle$and $|i\rangle$ of equation (29) as those of the Mn_1 ion, the expression leads to the susceptibility $\chi_{\alpha\beta\gamma}$ for a single ion of section 5.1. If we choose as P the sum of the dipole moments of Mn ions within a unit cell and as the states $|m\rangle$ those representing the coherent excitation transfer, i.e., the exciton states, equation (29) serves as the expression for χ per unit cell as will be shown in section 5.3.

The following relations which were important in the previous treatment [9, 10] are also found to be useful in the present calculation:

$$\langle R\psi|A|R\psi'\rangle = \langle\psi|R^{-1}AR|\psi'\rangle, \tag{32}$$

$$\langle\theta R\psi|A|\theta R\psi'\rangle = \langle\psi|\theta^{-1}R^{-1}AR\theta|\psi'\rangle^* \tag{33}$$

where A is a Hermitian operator, while R is any unitary symmetry operation such as C_3.

5.1. Single-ion theory

To calculate susceptibilities within the single-ion theory, we assume that $\chi_{\alpha\alpha\alpha}$ per unit cell ($\alpha = x$ or y) is given by the sum of the contributions $\chi_{\alpha\alpha\alpha}(i)$ ($i = 1, 2, \ldots, 6$) from the six ions Mn_i in the unit cell, so

$$\chi_{\alpha\alpha\alpha} = \sum_{i=1}^{3}\chi_{\alpha\alpha\alpha}(i) + \sum_{i=4}^{6}\chi_{\alpha\alpha\alpha}(i). \tag{34}$$

After some simple algebraic calculation using equations (1) and (2), we find

$$\sum_{i=1}^{3}\chi_{\alpha\alpha\alpha}(i) = \frac{3}{4}\left\{\chi_{\alpha\alpha\alpha}(1) - \sum\chi_{\alpha\beta\beta}(1)\right\} \tag{35}$$

where the sum on the right-hand side is defined by

$$\sum\chi_{\alpha\beta\beta}(1) = \chi_{\alpha\beta\beta}(1) + \chi_{\beta\alpha\beta}(1) + \chi_{\beta\beta\alpha}(1). \tag{36}$$

Note that $\beta = y$ when $\alpha = x$ and vice versa. In a similar way, we have

$$\sum_{i=4}^{6}\chi_{\alpha\alpha\alpha}(i) = \frac{3}{4}\left\{\chi_{\alpha\alpha\alpha}(4) - \sum\chi_{\alpha\beta\beta}(4)\right\}. \tag{37}$$

Now, in case (a), i.e., for $P6_3'cm'$, the operation $\sigma_d(\boldsymbol{\tau})$ with equation (32) leads to

$$\chi_{yyy}(4) = \chi_{yyy}(1) \qquad \chi_{yxx}(4) = \chi_{yxx}(1) \qquad \text{etc.} \tag{38}$$

In case (b), i.e., for $P6_3'c'm$, we have, similarly,

$$\chi_{xxx}(4) = -\chi^*_{xxx}(1) \qquad \chi_{xyy}(4) = -\chi^*_{xyy}(1) \qquad \text{etc} \tag{39}$$

with the aid of equation (33).

In case (a), only χ_{yyy} is non-vanishing. It is purely imaginary, because $\chi_{yyy}(1)$, etc, are themselves purely imaginary. In case (b), only χ_{xxx} is non-vanishing and purely imaginary, because only the imaginary parts of $\chi_{xxx}(1)$, etc, enter here. That is, we find for case (a) that the susceptibility per unit cell is expressed in terms of those for the ion Mn_1 as

$$\chi_{yyy} = \frac{3}{2}\left(\chi_{yyy}(1) - \sum \chi_{yxx}(1)\right) \tag{40}$$

and for the case (b), it may be written as

$$\chi_{xxx} = \mathrm{i}\frac{3}{2}\,\mathrm{Im}\left(\chi_{xxx}(1) - \sum \chi_{xyy}(1)\right). \tag{41}$$

An i-tensor χ_{zxx} has also been observed by Fröhlich *et al* [1]. With the $P6_3cm$ symmetry of the ferroelectric phase, the susceptibility χ_{zxx} for the unit cell is given by

$$\chi_{zxx} = 3(\chi_{zxx}(1) + \chi_{zyy}(1)) \tag{42}$$

in terms of the susceptibility for Mn_1. In a similar way, we find

$$\chi_{zzz} = 6\chi_{zzz}(1) \tag{43}$$

and

$$\chi_{xxz} = 3(\chi_{xxz}(1) + \chi_{yyz}(1)) \tag{44}$$

for other components of the i-tensor.

We note that the symmetry restrictions on the χ-tensor per unit cell result from those for the individual ions.

With these results, we now calculate the right-hand side of equation (31) for the ion Mn_1 and substitute the results obtained into the right-hand side of equations (40) and (41) given above. The components of the i-tensor may be obtained in a similar fashion.

As seen below, the susceptibilities obtained from the single-ion theory cannot actually explain all features of the observed SHG spectra. They certainly corroborate that the non-vanishing χ_{yyy} for case (a) and χ_{xxx} for case (b) are proportional, respectively, to the sublattice magnetizations (a) $\boldsymbol{S} \parallel \boldsymbol{x}$ and (b) $\boldsymbol{S} \parallel \boldsymbol{y}$. The expressions for the susceptibilities obtained predict, however, resonant SHG only at energies E_1 and E_2, while this is not the case for the observed spectra. Experimentally, two lines are found at the position of $E_2 \sim 2.45$ eV, and their interference behaviours in cases (a) and (b) are quite different—that is, constructive in case (a) and destructive in case (b). However, we are going into some detail in the calculation, because the results clearly suggest the possibility of a drastic difference in SHG accompanied by the rotation of the spin direction from $\boldsymbol{x}$ to $\boldsymbol{y}$ by 90°, and serve as an introduction to the treatment developed in the next subsection.

Starting from equations (40) and (41), we obtain the susceptibilities in the single-ion approximation as

$$\chi_{\alpha\alpha\alpha} = \chi^{(1)}_{\alpha\alpha\alpha} + \chi^{(2)}_{\alpha\alpha\alpha} \tag{45}$$

where $\alpha = x$ or y. As will be seen below, $\chi^{(1)}$ is proportional to the field $V(\mathrm{E_1a}) \propto zx$, while $\chi^{(2)}$ is to $V(\mathrm{B_2}) \propto z$.

The susceptibilities $\chi^{(1)}_{\alpha\alpha\alpha}$ are given by

(a)
$$\epsilon_0\chi^{(1)}_{yyy} = \frac{3}{2}\left[\frac{-(\hat{P}_y)_{01}(P_{2a})_{10}}{(E_1 - 2\hbar\omega)\,\Delta E} + \frac{(\hat{P}_x)_{02}(P_{2b})_{20}}{(E_2 - 2\hbar\omega)\,\Delta E}\right.$$
$$\left. + \frac{(P_x)_{01}(\hat{P}_{2b})_{10}}{(E_1 - 2\hbar\omega)\,\Delta E} + \frac{-(P_y)_{02}(\hat{P}_{2a})_{20}}{(E_2 - 2\hbar\omega)\,\Delta E}\right] \tag{46}$$

and

(b) $$\epsilon_0\chi^{(1)}_{xxx} = \mathrm{i}\frac{3}{2}\,\mathrm{Im}\left[\frac{(\hat{P}_x)_{01}(P_{2\mathrm{a}})_{10}}{(E_1-2\hbar\omega)\,\Delta E}+\frac{(\hat{P}_y)_{02}(P_{2\mathrm{b}})_{20}}{(E_2-2\hbar\omega)\,\Delta E}\right.$$
$$\left.+\frac{(P_x)_{01}(\hat{P}_{2\mathrm{a}})_{10}}{(E_1-2\hbar\omega)\,\Delta E}+\frac{(P_y)_{02}(\hat{P}_{2\mathrm{b}})_{20}}{(E_2-2\hbar\omega)\,\Delta E}\right] \tag{47}$$

where we have denoted, for example, the matrix elements of P_y connecting Ψ_0 and Ψ_1 perturbed by the spin–orbit interaction as $(\hat{P}_y)_{01}$, etc; these are called the spin-dependent transition moments.

The spin-dependent transition moments are given by

$$(\hat{P}_y)_{01} = +\langle \mathrm{A}_1|P_y|\mathrm{E}_2\mathrm{b}\rangle \mathrm{i}\lambda c\langle S_x\rangle/\Delta E(1,4) \tag{48}$$
$$(\hat{P}_x)_{02} = +\langle \mathrm{A}_1|P_x|\mathrm{E}_2\mathrm{a}\rangle \mathrm{i}\lambda c\langle S_x\rangle/\Delta E(2,3) \tag{49}$$
$$(\hat{P}_x)_{01} = +\langle \mathrm{A}_1|P_x|\mathrm{E}_2\mathrm{a}\rangle \mathrm{i}\lambda c\langle S_y\rangle/\Delta E(1,3) \tag{50}$$
$$(\hat{P}_y)_{02} = -\langle \mathrm{A}_1|P_y|\mathrm{E}_2\mathrm{b}\rangle \mathrm{i}\lambda c\langle S_y\rangle/\Delta E(2,4). \tag{51}$$

Anticipating the final result, we have replaced here the spin operators $S_{x,y}$ by their thermal averages $\langle S_{x,y}\rangle$ in the ground state, which are essentially the sublattice magnetizations in cases (a), (b). To show that this is a valid procedure is not so difficult, if we examine the expressions for the susceptibilities to be derived later, and remember that the excitation energies are assumed to be independent of the spin directions in the present treatment.

The operators $P_{2\mathrm{a}}$ and $P_{2\mathrm{b}}$ which transform like the bases $\mathrm{E}_2\mathrm{a}$ and $\mathrm{E}_2\mathrm{b}$ are defined by

$$P_{2\mathrm{a}} = P_x^2 - P_y^2 \tag{52}$$
$$P_{2\mathrm{b}} = -2P_xP_y \tag{53}$$

and their matrix elements are given by

$$(P_{2\mathrm{a}})_{10} = (\langle \mathrm{E}_1\mathrm{a}|V_m|\mathrm{E}_2\mathrm{a}\rangle/\Delta E(1,3))\langle \mathrm{E}_2\mathrm{a}|P_{2\mathrm{a}}|\mathrm{A}_1\rangle \tag{54}$$
$$(P_{2\mathrm{b}})_{20} = (\langle \mathrm{E}_1\mathrm{b}|V_m|\mathrm{E}_2\mathrm{b}\rangle/\Delta E(2,4))\langle \mathrm{E}_2\mathrm{b}|P_{2\mathrm{b}}|\mathrm{A}_1\rangle. \tag{55}$$

The spin-independent transition moments are obtained as

$$(P_x)_{01} = \langle\Psi_0|P_x|\Psi_1\rangle = \langle \mathrm{A}_1|P_x|\mathrm{E}_2\mathrm{a}\rangle\langle \mathrm{E}_2\mathrm{a}|V_m|\mathrm{E}_1\mathrm{a}\rangle/\Delta E(1,3) \tag{56}$$
$$(P_y)_{02} = \langle\Psi_0|P_y|\Psi_2\rangle = \langle \mathrm{A}_1|P_y|\mathrm{E}_2\mathrm{b}\rangle\langle \mathrm{E}_2\mathrm{b}|V_m|\mathrm{E}_1\mathrm{b}\rangle/\Delta E(2,4). \tag{57}$$

For $\chi^{(2)}_{\alpha\alpha\alpha}$, we have

(a) $$\epsilon_0\chi^{(2)}_{yyy} = \frac{3}{2}\left[\frac{(\bar{P}_x)_{01}(\hat{P}_{2\mathrm{b}})_{10}}{(E_1-2\hbar\omega)\,\Delta E}+\frac{-(\bar{P}_y)_{02}(\hat{P}_{2\mathrm{a}})_{20}}{(E_2-2\hbar\omega)\,\Delta E}\right] \tag{58}$$

and

(b) $$\epsilon_0\chi^{(2)}_{xxx} = \mathrm{i}\frac{3}{2}\,\mathrm{Im}\left[\frac{(\bar{P}_x)_{01}(\hat{P}_{2\mathrm{a}})_{10}}{(E_1-2\hbar\omega)\,\Delta E}+\frac{(\bar{P}_y)_{02}(\hat{P}_{2\mathrm{b}})_{20}}{(E_2-2\hbar\omega)\,\Delta E}\right]. \tag{59}$$

The matrix elements of $\hat{P}_{2\mathrm{a}}$, etc, are given by

$$(\hat{P}_{2\mathrm{b}})_{10} = -\mathrm{i}(\lambda c\langle S_x\rangle/\Delta E(1,4))\langle \mathrm{E}_2\mathrm{b}|P_{2\mathrm{b}}|\mathrm{A}_1\rangle \tag{60}$$
$$(\hat{P}_{2\mathrm{a}})_{20} = -\mathrm{i}(\lambda c\langle S_x\rangle/\Delta E(2,3))\langle \mathrm{E}_2\mathrm{a}|P_{2\mathrm{a}}|\mathrm{A}_1\rangle \tag{61}$$
$$(\hat{P}_{2\mathrm{a}})_{10} = -\mathrm{i}(\lambda c\langle S_y\rangle/\Delta E(1,3))\langle \mathrm{E}_2\mathrm{a}|P_{2\mathrm{a}}|\mathrm{A}_1\rangle \tag{62}$$
$$(\hat{P}_{2\mathrm{b}})_{20} = +\mathrm{i}(\lambda c\langle S_y\rangle/\Delta E(2,4))\langle \mathrm{E}_2\mathrm{b}|P_{2\mathrm{b}}|\mathrm{A}_1\rangle. \tag{63}$$

We have another kind of spin-independent transition moment appearing in $\chi^{(2)}_{\alpha\alpha\alpha}$:

$$(\bar{P}_x)_{01} = \langle\Psi_0|\bar{P}_x|\Psi_1\rangle = -\langle \mathrm{A}_1|V_m|\Phi_z\rangle\langle\Phi_z|P_x|\mathrm{E}_1\mathrm{a}\rangle/\Delta E_z \tag{64}$$

$$(\bar{P}_y)_{02} = \langle\Psi_0|\bar{P}_y|\Psi_2\rangle = -\langle \mathrm{A}_1|V_m|\Phi_z\rangle\langle\Phi_z|P_y|\mathrm{E}_1\mathrm{b}\rangle/\Delta E_z. \tag{65}$$

Matrix elements of orbital operators appearing in the susceptibilities will now be expressed in terms of the parameters defined through the following equations:

$$\langle \mathrm{A}_1|P_x|\Phi_x\rangle = \langle \mathrm{A}_1|P_y|\Phi_y\rangle = p \tag{66}$$

$$\langle\Phi_{x^2-y^2}|V(\mathrm{E}_1\mathrm{a})|\mathrm{E}_1\mathrm{a}\rangle = -\langle\Phi_{-2xy}|V(\mathrm{E}_1\mathrm{a})|\mathrm{E}_1\mathrm{b}\rangle = v_{zx} \tag{67}$$

$$\langle\Phi_x|V(\mathrm{B}_2)|\mathrm{E}_1\mathrm{a}\rangle = \langle\Phi_y|V(\mathrm{B}_2)|\mathrm{E}_1\mathrm{b}\rangle = v_z \tag{68}$$

$$\langle \mathrm{E}_2\mathrm{a}|V(\mathrm{E}_2\mathrm{a})|\mathrm{E}_1\mathrm{a}\rangle = \langle \mathrm{E}_2\mathrm{b}|V(\mathrm{E}_2\mathrm{a})|\mathrm{E}_1\mathrm{b}\rangle = 0 \tag{69}$$

$$\langle\Phi_{x^2-y^2}|P_{2\mathrm{a}}|\mathrm{A}_1\rangle = \langle\Phi_{-2xy}|P_{2\mathrm{b}}|\mathrm{A}_1\rangle = q \tag{70}$$

$$\langle \mathrm{A}_1|V(\mathrm{B}_2)|\Phi_z\rangle = \bar{v}_z \tag{71}$$

$$\langle\Phi_z|P_x|\mathrm{E}_1\mathrm{a}\rangle = \langle\Phi_z|P_y|\mathrm{E}_1\mathrm{b}\rangle = \bar{p}. \tag{72}$$

In deriving these relations, we have kept in mind the reduction of the product representations given by

$$\mathrm{E}_1\times\mathrm{E}_1 = \mathrm{A}_1+\mathrm{A}_2+\mathrm{E}_2 \tag{73}$$

$$\mathrm{E}_2\times\mathrm{E}_2 = \mathrm{A}_1+\mathrm{A}_2+\mathrm{E}_2 \tag{74}$$

$$\mathrm{E}_1\times\mathrm{E}_2 = \mathrm{B}_2+\mathrm{B}_1+\mathrm{E}_1 \tag{75}$$

together with the Wigner–Eckart theorem [7].

With a simplifying assumption that terms proportional to c'^2 may be neglected, we are able to calculate χ, i.e., the right-hand side of equations (46) and (47), in terms of the parameters defined above, and the results are

(a) $$\epsilon_0\chi^{(1)}_{yyy} = -\mathrm{i}\frac{3}{2}c^3c'pq\langle S_x\rangle \times\left[\frac{(\lambda/\Delta E(1,4))v_{zx}/\Delta E(1,3)+(v_{zx}/\Delta E(1,3))\lambda/\Delta E(1,4)}{(E_1-2\hbar\omega)\,\Delta E} + \frac{(\lambda/\Delta E(2,3))v_{zx}/\Delta E(2,4)+(v_{zx}/\Delta E(2,4))\lambda/\Delta E(2,3)}{(E_2-2\hbar\omega)\,\Delta E}\right] \tag{76}$$

and

(b) $$\epsilon_0\chi^{(1)}_{xxx} = 0. \tag{77}$$

We thus find that the first line of equation (46) is equal to the second, so it is simply doubled, whereas that of equation (47) is cancelled by the second. Therefore, only $\chi^{(2)}_{xxx}$ remains in case (b).

The susceptibilities $\chi^{(2)}_{\alpha\alpha\alpha}$ are proportional to $\bar{v}_z$ and are given by

(a) $$\epsilon_0\chi^{(2)}_{yyy} = \mathrm{i}\frac{3}{2}c^2\frac{\bar{v}_z}{\Delta E_z}\bar{p}q\langle S_x\rangle\left[\frac{\lambda/\Delta E(1,4)}{(E_1-2\hbar\omega)\,\Delta E} - \frac{\lambda/\Delta E(2,3)}{(E_2-2\hbar\omega)\,\Delta E}\right] \tag{78}$$

and

(b) $$\epsilon_0\chi^{(2)}_{xxx} = \mathrm{i}\frac{3}{2}c^2\frac{\bar{v}_z}{\Delta E_z}\bar{p}q\langle S_y\rangle\left[\frac{\lambda/\Delta E(1,3)}{(E_1-2\hbar\omega)\,\Delta E} - \frac{\lambda/\Delta E(2,4)}{(E_2-2\hbar\omega)\,\Delta E}\right]. \tag{79}$$

According to equation (42), the expression for the i-tensor $\chi^{(i)}_{zxx}\equiv\chi_{zxx}$ is given by

$$\epsilon_0\chi_{zxx} = 3\frac{(P_z)_{01}(P_x^2+P_y^2)_{10}}{(E_1-2\hbar\omega)\,\Delta E}. \tag{80}$$

The matrix elements appearing here are given by

$$(P_z)_{01} = -\langle \mathrm{A}_1|P_z|\Phi_z\rangle\langle\Phi_z|V(\mathrm{E}_2\mathrm{a})|\mathrm{E}_1\mathrm{a}\rangle/\Delta E(z,1) - \langle \mathrm{A}_1|V(\mathrm{E}_2\mathrm{a})|\Psi_3\rangle\langle\Psi_3|P_z|\mathrm{E}_1\mathrm{a}\rangle/\Delta E(3,0) \tag{81}$$

and

$$(P_x^2+P_y^2)_{10} = \frac{\langle \mathrm{E}_1\mathrm{a}|V(\mathrm{E}_1\mathrm{a})|\mathrm{A}_1\rangle}{\Delta E(1,0)}\langle \mathrm{A}_1|P_x^2+P_y^2|\mathrm{A}_1\rangle. \tag{82}$$

The expression for χ_{zzz} takes the following form:

$$\epsilon_0\chi_{zzz} = 6\frac{(P_z)_{01}(P_z^2)_{10}}{(E_1-2\hbar\omega)\,\Delta E} \tag{83}$$

with

$$(P_z^2)_{10} = \frac{\langle \mathrm{E}_1\mathrm{a}|V(\mathrm{E}_1\mathrm{a})|\mathrm{A}_1\rangle}{\Delta E(1,0)}\langle \mathrm{A}_1|P_z^2|\mathrm{A}_1\rangle. \tag{84}$$

The component χ_{xxz} is given by

$$\epsilon_0\chi_{xxz} = 3\left\{\frac{(P_x)_{01}(P_xP_z)_{10}}{(E_1-2\hbar\omega)\,\Delta E} + \frac{(P_y)_{02}(P_yP_z)_{20}}{(E_2-2\hbar\omega)\,\Delta E}\right\}. \tag{85}$$

The matrix element $(P_x)_{10}$ here is given by the sum of the right-hand sides of equations (56) and (64), and $(P_y)_{20}$ is given by the sum of those of equations (57) and (65). We also find

$$(P_xP_z)_{10} = \langle \mathrm{E}_1\mathrm{a}|P_xP_z|\mathrm{A}_1\rangle \tag{86}$$

$$(P_yP_z)_{20} = \langle \mathrm{E}_1\mathrm{b}|P_yP_z|\mathrm{A}_1\rangle. \tag{87}$$

Note that the fields $V(\mathrm{E}_1\mathrm{a})$ and $V(\mathrm{B}_2)$ change sign when operated on by σ_h (reflection in the xy-plane, $z \to -z$). This corresponds to the change in the sign of χ_{zxx}, etc, when one goes over from one ferroelectric domain to another.

Let us derive, finally, the expression for the susceptibility corresponding to the resonant SHG at energies E_3 and E_4. Corresponding to equation (46), we have

$$\text{(a)}\qquad \epsilon_0\chi_{yyy} = \frac{3}{2}\left[\frac{-(\hat{P}_y)_{03}(P_{2\mathrm{a}})_{30}}{(E_3-2\hbar\omega)\,\Delta E} + \frac{(\hat{P}_x)_{04}(P_{2\mathrm{b}})_{40}}{(E_4-2\hbar\omega)\,\Delta E} + \frac{(P_x)_{03}(\hat{P}_{2\mathrm{b}})_{30}}{(E_3-2\hbar\omega)\,\Delta E} + \frac{-(P_y)_{04}(\hat{P}_{2\mathrm{a}})_{40}}{(E_4-2\hbar\omega)\,\Delta E}\right] \tag{88}$$

where

$$(\hat{P}_y)_{03} = +\langle \mathrm{A}_1|P_y|\mathrm{E}_2\mathrm{b}\rangle(-2\mathrm{i})\lambda c^2\langle S_z\rangle/\Delta E(3,4) \tag{89}$$

$$(\hat{P}_x)_{04} = -\langle \mathrm{A}_1|P_x|\mathrm{E}_2\mathrm{a}\rangle 2\mathrm{i}\lambda c^2\langle S_z\rangle/\Delta E(3,4) \tag{90}$$

and

$$(\hat{P}_{2\mathrm{b}})_{30} = 2\mathrm{i}(\lambda c^2\langle S_z\rangle/\Delta E(3,4))\langle \mathrm{E}_2\mathrm{b}|P_{2\mathrm{b}}|\mathrm{A}_1\rangle \tag{91}$$

$$(\hat{P}_{2\mathrm{a}})_{40} = 2\mathrm{i}(\lambda c^2\langle S_z\rangle/\Delta E(3,4))\langle \mathrm{E}_2\mathrm{a}|P_{2\mathrm{a}}|\mathrm{A}_1\rangle. \tag{92}$$

It is easy to show that $(P_x)_{03} = (P_y)_{04} = c'p$ and $(P_{2\mathrm{a}})_{30} = (P_{2\mathrm{b}})_{40} = cq$, so we obtain

$$\text{(a)}\qquad \epsilon_0\chi_{yyy} = \mathrm{i}\frac{3}{2}c^3c'pq\langle S_z\rangle\left[\frac{2\lambda/\Delta E(3,4)}{(E_3-2\hbar\omega)\,\Delta E} - \frac{2\lambda/\Delta E(3,4)}{(E_4-2\hbar\omega)\,\Delta E}\right] \tag{93}$$

which is proportional to $\langle S_z\rangle$. This suggests that canting of the spins in this case may be confirmed by the observation of SHG at E_3 and E_4. Note also that χ_{yyy} here is independent of the direction of the electric polarization, unlike the susceptibilities at E_1 and E_2.

Examination of the expression for χ_{xxx} shows that

$$\text{(b)} \qquad \epsilon_0 \chi_{xxx} = 0 \tag{94}$$

under the same approximation, in accordance with the vanishing of $\langle S_z \rangle$ in case (b).

An expression similar to equation (85) can be obtained for χ_{xxz} at E_3 and E_4 by replacing (Ψ_1, E_1) and (Ψ_2, E_2) by (Ψ_3, E_3) and (Ψ_4, E_4), respectively.

5.2. Exciton theory

Since the single-ion theory does not work well, as pointed out in the paragraph preceding the one containing equation (45), we consider in this subsection the effect of excitation transfer among the Mn ions and examine whether it can explain the observed features of the spectra.

The theory of Frenkel excitons in magnetic crystals is well developed [11]. We first give an outline of the theory, simply because we need to explain the notation adopted in this subsection.

The ground state of the whole system is described as

$$\Psi_g = \prod_{n\beta} \psi_{n\beta} \tag{95}$$

where $\psi_{n\beta}$ represents the ground state of the Mn ion at the β (=1, ..., 6) site of the nth cell. The ground-state wave function $\psi_{0\,\beta=1}$ behaves like $z^2(\Gamma_1)$ under σ_v. When one of the Mn ions, i.e., the one at $(m\alpha)$, is excited to the state $\psi_{m\alpha\lambda}$, we have the localized excited state

$$\Psi_{m\alpha\lambda} = \psi_{m\alpha\lambda} \prod_{n\beta}{}' \psi_{n\beta} \tag{96}$$

where the prime on the symbol for the product indicates that the case $n\beta = m\alpha$ is to be excluded. The excited-state wave functions for Mn_1 in the 0th cell, $\psi_{m=0\,\alpha=1\,\lambda=1,2}$, are the states $\Psi_{1,2}$ of section 3, which are perturbed by V_m as well as the spin–orbit interaction. Their unperturbed orbital parts transform like $zx(\Gamma_1)$ and zy (Γ_2), respectively.

Then, the exciton states at the Γ point ($\boldsymbol{k} = 0$) are given by

$$\Psi_\lambda(\alpha) = \frac{1}{\sqrt{N}} \sum_m \Psi_{m\alpha\lambda} \tag{97}$$

where N represents the number of unit cells. The matrix elements of the Hamiltonian involving the excitation transfer can be calculated as

$$\begin{aligned}\mathcal{H}_{\alpha\lambda,\alpha'\lambda'} &= \langle \Psi_\lambda(\alpha) | \mathcal{H} | \Psi_{\lambda'}(\alpha') \rangle \\ &= \sum_n \langle \Psi_{m=0\alpha\lambda} | \mathcal{H} | \Psi_{n\alpha'\lambda'} \rangle = \sum_n \langle \psi_{0\alpha\lambda} \psi_{n\alpha'} | W_{0\alpha,n\alpha'} | \psi_{0\alpha} \psi_{n\alpha'\lambda'} \rangle\end{aligned} \tag{98}$$

and the excited eigenstates are obtained from

$$\Psi_i = \sum_{\alpha\lambda} \Psi_\lambda(\alpha) c^i_{\alpha\lambda}. \tag{99}$$

The coefficients $c^i_{\alpha\lambda}$ are determined from

$$\sum_{\alpha'\lambda'} \mathcal{H}_{\alpha\lambda,\alpha'\lambda'} c^i_{\alpha'\lambda'} = E_i c^i_{\alpha\lambda}. \tag{100}$$

In equation (98), the interaction $W_{0\alpha,n\alpha'}$ describes the transfer of excitation between ions at (0α) and $(n\alpha')$, i.e., the de-excitation from the excited state λ' at $(n\alpha')$ and excitation to the excited state λ at (0α). The derivation of this interaction and its explicit expression are given in the appendix.

According to equation (A.17), for example, in equation (98)

$$W_{01,n2} = k_{x\xi} w(1y, 2\eta) + k_{y\eta} w(1x, 2\xi) - k_{x\eta} w(1y, 2\xi) - k_{y\xi} w(1x, 2\eta). \tag{101}$$

Making use of equation (A.21) and similar equations, we obtain $(\mathcal{H})_{\alpha\lambda,\alpha'\lambda}$ $(\lambda = 1, 2)$:

$$
\begin{array}{cc}
 & \begin{array}{cccccc} 1 & 2 & 3 & 4 & 5 & 6 \end{array} \\
\begin{array}{c} 1 \\ 2 \\ 3 \\ 4 \\ 5 \\ 6 \end{array} &
\begin{pmatrix}
0 & -K_\lambda & -K_\lambda & -K'_\lambda & \overline{K}_\lambda & \overline{K}_\lambda \\
-K_\lambda & 0 & -K_\lambda & \overline{K}_\lambda & -K'_\lambda & \overline{K}_\lambda \\
-K_\lambda & -K_\lambda & 0 & \overline{K}_\lambda & \overline{K}_\lambda & -K'_\lambda \\
-K'_\lambda & \overline{K}_\lambda & \overline{K}_\lambda & 0 & -K_\lambda & -K_\lambda \\
\overline{K}_\lambda & -K'_\lambda & \overline{K}_\lambda & -K_\lambda & 0 & -K_\lambda \\
\overline{K}_\lambda & \overline{K}_\lambda & -K'_\lambda & -K_\lambda & -K_\lambda & 0
\end{pmatrix}
\end{array}
\tag{102}
$$

where

$$K_1 = -F_{12} \sum_n k_{x\xi}(01, n2) \qquad K_2 = -F_{12} \sum_n k_{y\eta}(01, n2) \tag{103}$$

$$K'_1 = -F_{14} \sum_n k_{x\xi}(01, n4) \qquad K'_2 = -F_{14} \sum_n k_{y\eta}(01, n4) \tag{104}$$

$$\overline{K}_1 = F_{15} \sum_n k_{x\xi}(01, n5) \qquad \overline{K}_2 = F_{15} \sum_n k_{y\eta}(01, n5) \tag{105}$$

and we have $(\mathcal{H})_{\alpha 1,\alpha' 2} = (\mathcal{H})_{\alpha' 2,\alpha 1}$:

$$
\begin{array}{cc}
 & \begin{array}{cccccc} 1 & 2 & 3 & 4 & 5 & 6 \end{array} \\
\begin{array}{c} 1 \\ 2 \\ 3 \\ 4 \\ 5 \\ 6 \end{array} &
\begin{pmatrix}
0 & -\sqrt{3}K & \sqrt{3}K & 0 & \sqrt{3}\,\overline{K} & -\sqrt{3}\,\overline{K} \\
\sqrt{3}K & 0 & -\sqrt{3}K & -\sqrt{3}\,\overline{K} & 0 & \sqrt{3}\,\overline{K} \\
-\sqrt{3}K & \sqrt{3}K & 0 & \sqrt{3}\,\overline{K} & -\sqrt{3}\,\overline{K} & 0 \\
0 & \sqrt{3}\,\overline{K} & -\sqrt{3}\,\overline{K} & 0 & -\sqrt{3}K & \sqrt{3}K \\
-\sqrt{3}\,\overline{K} & 0 & \sqrt{3}\,\overline{K} & \sqrt{3}K & 0 & -\sqrt{3}K \\
\sqrt{3}\,\overline{K} & -\sqrt{3}\,\overline{K} & 0 & -\sqrt{3}K & \sqrt{3}K & 0
\end{pmatrix}
\end{array}
\tag{106}
$$

where

$$K = -\frac{1}{\sqrt{3}} F_{12} \sum_n k_{x\eta}(01, n2) \tag{107}$$

$$\overline{K} = \frac{1}{\sqrt{3}} F_{15} \sum_n k_{x\eta}(01, n5). \tag{108}$$

Apparently, the 12-dimensional matrix $\mathcal{H}_{\alpha\lambda,\alpha'\lambda'}$ has the symmetry of C_{6v}, so its diagonalization is made easy by making linear combinations of $\Psi_\lambda(\alpha)$ corresponding to the irreducible representations of C_{6v} given in table 1.

Table 1. The character table for C_{6v}; (a) $6'mm'$, (b) $6'm'm$.

(a)	E	$2\theta C_6(\tau)$	$2C_3$	$\theta C_2(\tau)$	$3\sigma_d(\tau)$	$3\theta\sigma_v$	
(b)	E	$2\theta C_6(\tau)$	$2C_3$	$\theta C_2(\tau)$	$3\theta\sigma_d(\tau)$	$3\sigma_v$	
A_1	1	1	1	1	1	1	z
A_2	1	1	1	1	−1	−1	$x_1y_2 - y_1x_2$
B_1	1	−1	1	−1	1	−1	$y^3 - 3x^2y$
B_2	1	−1	1	−1	−1	1	$x^3 - 3xy^2$
E_1	2	1	−1	−2	0	0	(x, y)
E_2	2	−1	−1	2	0	0	$(2xy, x^2 - y^2)$

We first set

$$\Psi_{1\pm}(\mathrm{A}) = \frac{1}{\sqrt{6}}(\Psi_1(1)+\Psi_1(2)+\Psi_1(3)) \pm \frac{1}{\sqrt{6}}(\Psi_1(4)+\Psi_1(5)+\Psi_1(6)) \tag{109}$$

$$\Psi_{1\pm}(\mathrm{E}x) = \frac{1}{2\sqrt{3}}(2\Psi_1(1)-\Psi_1(2)-\Psi_1(3)) \pm \frac{1}{2\sqrt{3}}(2\Psi_1(4)-\Psi_1(5)-\Psi_1(6)) \tag{110}$$

$$\Psi_{1\pm}(\mathrm{E}y) = \frac{1}{2}(\Psi_1(2)-\Psi_1(3)) \pm \frac{1}{2}(\Psi_1(5)-\Psi_1(6)) \tag{111}$$

$$\Psi_{2\pm}(\mathrm{A}) = \frac{1}{\sqrt{6}}(\Psi_2(1)+\Psi_2(2)+\Psi_2(3)) \pm \frac{1}{\sqrt{6}}(\Psi_2(4)+\Psi_2(5)+\Psi_2(6)) \tag{112}$$

$$\Psi_{2\pm}(\mathrm{E}x) = \frac{1}{2}(-\Psi_2(2)+\Psi_2(3)) \pm \frac{1}{2}(-\Psi_2(5)+\Psi_2(6)) \tag{113}$$

$$\Psi_{2\pm}(\mathrm{E}y) = \frac{1}{2\sqrt{3}}(2\Psi_2(1)-\Psi_2(2)-\Psi_2(3)) \pm \frac{1}{2\sqrt{3}}(2\Psi_2(4)-\Psi_2(5)-\Psi_2(6)). \tag{114}$$

The symmetry-adapted functions are then given by

$$\begin{array}{ll}
\Psi(\mathrm{A}_1) \equiv \Psi_{1+}(\mathrm{A}) & \Psi(\mathrm{B}_2) \equiv \Psi_{1-}(\mathrm{A}) \\
\Psi_1(\mathrm{E}_2x) \equiv \Psi_{1+}(\mathrm{E}y) & \Psi_1(\mathrm{E}_1x) \equiv \Psi_{1-}(\mathrm{E}x) \\
\Psi_1(\mathrm{E}_2y) \equiv -\Psi_{1+}(\mathrm{E}x) & \Psi_1(\mathrm{E}_1y) \equiv \Psi_{1-}(\mathrm{E}y) \\
\Psi(\mathrm{A}_2) \equiv \Psi_{2+}(\mathrm{A}) & \Psi(\mathrm{B}_1) \equiv \Psi_{2-}(\mathrm{A}) \\
\Psi_2(\mathrm{E}_2x) \equiv \Psi_{2+}(\mathrm{E}y) & \Psi_2(\mathrm{E}_1x) \equiv \Psi_{2-}(\mathrm{E}x) \\
\Psi_2(\mathrm{E}_2y) \equiv -\Psi_{2+}(\mathrm{E}x) & \Psi_2(\mathrm{E}_1y) \equiv \Psi_{2-}(\mathrm{E}y)
\end{array}$$

where the symmetry labels are given as the arguments of the functions on the left-hand side.

This shows that the 12-dimensional secular determinant for $\mathcal{H}_{\alpha\lambda,\alpha'\lambda'}$ will be factorized into eight factors: four one-dimensional A_1, B_2, A_2, B_1, two two-dimensional E_2x and E_1x, and two two-dimensional E_2y and E_1y ones.

The exciton energies for the four one-dimensional representations are easily found:

$$E(\mathrm{A}_1) = E_1 - 2K_1 - K_1' + 2\overline{K}_1 \qquad E(\mathrm{B}_2) = E_1 - 2K_1 + K_1' - 2\overline{K}_1 \tag{115}$$

$$E(\mathrm{A}_2) = E_2 - 2K_2 - K_2' + 2\overline{K}_2 \qquad E(\mathrm{B}_1) = E_2 - 2K_2 + K_2' - 2\overline{K}_2. \tag{116}$$

The two eigenvalues of $E(\mathrm{E}_2y)$ (and $E(\mathrm{E}_2x)$) are obtained from the diagonalization of

$$\begin{array}{cc}
 & \begin{array}{cc} \Psi_1(\mathrm{E}_2y) \qquad\qquad & \Psi_2(\mathrm{E}_2y) \end{array} \\
\begin{array}{c} \Psi_1(\mathrm{E}_2y) \\ \Psi_2(\mathrm{E}_2y) \end{array} & \begin{pmatrix} E_1 + K_1 - K_1' - \overline{K}_1 & 3K - 3\overline{K} \\ 3K - 3\overline{K} & E_2 + K_2 - K_2' - \overline{K}_2 \end{pmatrix}
\end{array} \tag{117}$$

with the eigenfunctions:

$$\Psi(\nu\mathrm{E}_2) = \nu_1\Psi_1(\mathrm{E}_2y) + \nu_2\Psi_2(\mathrm{E}_2y). \tag{118}$$

Hereafter, the lower- and higher-energy E_2 states will be distinguished by $\nu = -$ and $\nu = +$, respectively.

Similarly, the two eigenvalues of $E(\mathrm{E}_1y)$ (and $E(\mathrm{E}_1x)$) are obtained from the diagonalization of

$$\begin{array}{cc}
 & \begin{array}{cc} \Psi_1(\mathrm{E}_1y) \qquad\qquad & \Psi_2(\mathrm{E}_1y) \end{array} \\
\begin{array}{c} \Psi_1(\mathrm{E}_1y) \\ \Psi_2(\mathrm{E}_1y) \end{array} & \begin{pmatrix} E_1 + K_1 + K_1' + \overline{K}_1 & 3K + 3\overline{K} \\ 3K + 3\overline{K} & E_2 + K_2 + K_2' + \overline{K}_2 \end{pmatrix}
\end{array} \tag{119}$$

with

$$\Psi(\mu\mathrm{E}_1) = \mu_1\Psi_1(\mathrm{E}_1y) + \mu_2\Psi_2(\mathrm{E}_1y). \tag{120}$$

We also associate $\mu = -$ and $\mu = +$ with the lower-energy and higher-energy eigenvalues obtained here.

At this stage, we see a possible interpretation of the structures of the observed SHG χ_{xxx}-spectra, for example. We expect a pair of lines near each pair of energies E_1 and E_2 of the single-ion theory. The two lines on the lower-energy side ($\sim E_2$) are likely to correspond to ($\mu = -, \mathrm{E}_1$) and ($\nu = -, \mathrm{E}_2$), while the other two lines with higher energy ($\sim E_1$) may be associated with ($\mu = +, \mathrm{E}_1$) and ($\nu = +, \mathrm{E}_2$). As will be seen in the next subsection, all four states are optically accessible.

5.3. Susceptibilities in exciton modes

The transition moments involved may be calculated as follows:

$$\langle\Psi_g|P_y|\Psi_i\rangle = \sum_{\alpha\lambda}\langle\Psi_g|P_y|\Psi_\lambda(\alpha)\rangle c^i_{\alpha\lambda} = \sqrt{N}\sum_{\alpha\lambda}\langle\psi_{0\alpha}|p_y|\psi_{0\alpha\lambda}\rangle c^i_{\alpha\lambda} \tag{121}$$

and

$$\langle\Psi_i|P_yP_y|\Psi_g\rangle = \sqrt{N}\sum_{\alpha\lambda}(c^i_{\alpha\lambda})^*\langle\psi_{0\alpha\lambda}|p_yp_y|\psi_{0\alpha}\rangle. \tag{122}$$

The following identities are conveniently used to correlate the matrix elements evaluated at different sites:

$$R_\vartheta(z)p_xR_\vartheta^{-1}(z) = p_x\cos\vartheta + p_y\sin\vartheta \tag{123}$$

$$R_\vartheta(z)p_yR_\vartheta^{-1}(z) = -p_x\sin\vartheta + p_y\cos\vartheta \tag{124}$$

where, for example, $R_{2\pi/3}(z) = C_3$.

The susceptibilities of the system are now given by

$$\text{(a)}\qquad \epsilon_0N\chi^{(1)}_{yyy} = \sum_\nu\frac{\langle\Psi_g|P_y|\Psi(\nu\mathrm{E}_2)\rangle\langle\Psi(\nu\mathrm{E}_2)|P_yP_y|\Psi_g\rangle}{(E(\nu\mathrm{E}_2)-2\hbar\omega)\,\Delta E} + \sum_\mu\frac{\langle\Psi_g|P_y|\Psi(\mu\mathrm{E}_1)\rangle\langle\Psi(\mu\mathrm{E}_1)|P_yP_y|\Psi_g\rangle}{(E(\mu\mathrm{E}_1)-2\hbar\omega)\Delta E} \tag{125}$$

$$\text{(b)}\qquad \epsilon_0N\chi^{(1)}_{xxx} = \sum_\nu\frac{\langle\Psi_g|P_x|\Psi(\nu\mathrm{E}_2)\rangle\langle\Psi(\nu\mathrm{E}_2)|P_xP_x|\Psi_g\rangle}{(E(\nu\mathrm{E}_2)-2\hbar\omega)\,\Delta E} + \sum_\mu\frac{\langle\Psi_g|P_x|\Psi(\mu\mathrm{E}_1)\rangle\langle\Psi(\mu\mathrm{E}_1)|P_xP_x|\Psi_g\rangle}{(E(\mu\mathrm{E}_1)-2\hbar\omega)\,\Delta E}. \tag{126}$$

The transition moments appearing in these equations may be obtained, after somewhat tedious calculations, by means of equations (121) and (122), as

$$\begin{aligned}\langle\Psi_g|P_y|\Psi(\nu\mathrm{E}_2)\rangle/\sqrt{N} &= -\sqrt{3}((\hat{P}_y)_{01}\,\nu_1 - (\hat{P}_x)_{02}\,\nu_2)\\ \langle\Psi_g|P_y|\Psi(\mu\mathrm{E}_1)\rangle/\sqrt{N} &= \sqrt{3}((P_x)_{01}\,\mu_1 + (P_y)_{02}\,\mu_2)\end{aligned} \tag{127}$$

and

$$\begin{aligned}\langle\Psi(\nu\mathrm{E}_2)|P_yP_y|\Psi_g\rangle/\sqrt{N} &= \frac{\sqrt{3}}{2}((P_{2\mathrm{a}})_{10}\,\nu_1 + (P_{2\mathrm{b}})_{20}\,\nu_2)\\ \langle\Psi(\mu\mathrm{E}_1)|P_yP_y|\Psi_g\rangle/\sqrt{N} &= \frac{\sqrt{3}}{2}((\hat{P}_{2\mathrm{b}})_{10}\,\mu_1 - (\hat{P}_{2\mathrm{a}})_{20}\,\mu_2)\end{aligned} \tag{128}$$

in terms of the matrix elements which appeared in the single-ion theory[1].

Similarly, we find

$$\begin{aligned}\langle\Psi_g|P_x|\Psi(\nu E_2)\rangle/\sqrt{N} &= -i\sqrt{3}\,\mathrm{Im}((\hat{P}_x)_{01}\,\nu_1 + (\hat{P}_y)_{02}\,\nu_2)\\ \langle\Psi_g|P_x|\Psi(\mu E_1)\rangle/\sqrt{N} &= \sqrt{3}\,\mathrm{Re}((P_x)_{01}\,\mu_1 + (P_y)_{02}\,\mu_2)\end{aligned} \tag{129}$$

and

$$\begin{aligned}\langle\Psi(\nu E_2)|P_xP_x|\Psi_g\rangle/\sqrt{N} &= -\frac{\sqrt{3}}{2}\,\mathrm{Re}((P_{2a})_{10}\,\nu_1 + (P_{2b})_{20}\,\nu_2)\\ \langle\Psi(\mu E_1)|P_xP_x|\Psi_g\rangle/\sqrt{N} &= i\frac{\sqrt{3}}{2}\,\mathrm{Im}((\hat{P}_{2a})_{10}\,\mu_1 + (\hat{P}_{2b})_{20}\,\mu_2)\end{aligned} \tag{130}$$

where we choose the E_1x component on the right-hand side of equation (120) for $\Psi(\mu E_1)$ instead of the E_1y component. We thus have

$$\text{(a)}\qquad \begin{aligned}\epsilon_0\chi^{(1)}_{yyy} &= \frac{3}{2}\sum_\nu \frac{-((\hat{P}_y)_{01}\,\nu_1 - (\hat{P}_x)_{02}\,\nu_2)((P_{2a})_{10}\,\nu_1 + (P_{2b})_{20}\,\nu_2)}{(E(\nu E_2) - 2\hbar\omega)\,\Delta E}\\ &\quad + \frac{3}{2}\sum_\mu \frac{((P_x)_{01}\,\mu_1 + (P_y)_{02}\,\mu_2)((\hat{P}_{2b})_{10}\,\mu_1 - (\hat{P}_{2a})_{20}\,\mu_2)}{(E(\mu E_1) - 2\hbar\omega)\,\Delta E}\end{aligned} \tag{131}$$

and

$$\text{(b)}\qquad \begin{aligned}\epsilon_0\chi^{(1)}_{xxx} &= i\frac{3}{2}\sum_\nu \frac{\mathrm{Im}((\hat{P}_x)_{01}\,\nu_1 + (\hat{P}_y)_{02}\,\nu_2)\,\mathrm{Re}((P_{2a})_{10}\,\nu_1 + (P_{2b})_{20}\,\nu_2)}{(E(\nu E_2) - 2\hbar\omega)\,\Delta E}\\ &\quad + i\frac{3}{2}\sum_\mu \frac{\mathrm{Re}((P_x)_{01}\,\mu_1 + (P_y)_{02}\,\mu_2)\,\mathrm{Im}((\hat{P}_{2a})_{10}\,\mu_1 + (\hat{P}_{2b})_{20}\,\mu_2)}{(E(\mu E_1) - 2\hbar\omega)\,\Delta E}\end{aligned} \tag{132}$$

for the susceptibility per unit cell.

It is interesting to compare these results with those from the single-ion theory, i.e., equations (76) and (77).

Equation (131) may finally be written as

$$\text{(a)}\qquad \begin{aligned}\epsilon_0\chi^{(1)}_{yyy} &= -i\frac{3}{2}c^3c'pq\langle S_x\rangle\\ &\quad\times\Bigg[\sum_\nu \frac{(\nu_1\lambda/\Delta E(1,4) - \nu_2\lambda/\Delta E(2,3))}{(E(\nu E_2) - 2\hbar\omega)\,\Delta E}\\ &\quad\times(\nu_1 v_{zx}/\Delta E(1,3) - \nu_2 v_{zx}/\Delta E(2,4))\\ &\quad+\sum_\mu \frac{(\mu_1 v_{zx}/\Delta E(1,3) - \mu_2 v_{zx}/\Delta E(2,4))}{(E(\mu E_1) - 2\hbar\omega)\,\Delta E}\\ &\quad\times(\mu_1\lambda/\Delta E(1,4) - \mu_2\lambda/\Delta E(2,3))\Bigg].\end{aligned} \tag{133}$$

[1] Straightforward application of the Wigner–Eckart theorem to the calculation of the matrix element $\langle\Psi_g|P_y|\Psi(\nu E_2)\rangle$ on the first line of equation (127) and $\langle\Psi(\mu E_1)|P_yP_y|\Psi_g\rangle$ on the second line of equation (128) would seem to make the right-hand sides of these equations vanish. However, this is not correct, because both $\Psi(\nu E_2)$ and $\Psi(\mu E_1)$ are actually mixed with components brought in through the spin–orbit interaction. It is these perturbed parts that make the matrix elements in question non-vanishing, as suggested by the expressions on the right-hand side. The same remark applies to equations (129) and (130).

Similarly, equation (132) may be put in the form

$$\text{(b)} \qquad \epsilon_0 \chi^{(1)}_{xxx} = \mathrm{i}\frac{3}{2}c^3 c' pq \langle S_y \rangle \times \Bigg[\sum_{\nu} \frac{(\nu_1 \lambda/\Delta E(1,3) - \nu_2 \lambda/\Delta E(2,4))}{(E(\nu \mathrm{E}_2) - 2\hbar\omega)\,\Delta E} \times (\nu_1 v_{zx}/\Delta E(1,3) - \nu_2 v_{zx}/\Delta E(2,4)) - \sum_{\mu} \frac{(\mu_1 v_{zx}/\Delta E(1,3) - \mu_2 v_{zx}/\Delta E(2,4))}{(E(\mu \mathrm{E}_1) - 2\hbar\omega)\,\Delta E} \times (\mu_1 \lambda/\Delta E(1,3) - \mu_2 \lambda/\Delta E(2,4)) \Bigg]. \tag{134}$$

The susceptibilities proportional to $\bar{v}_z$ are calculated as

$$\text{(a)} \qquad \epsilon_0 \chi^{(2)}_{yyy} = \mathrm{i}\frac{3}{2}c^2 \frac{\bar{v}_z}{\Delta E_z} \bar{p} q \langle S_x \rangle \sum_{\mu} \frac{(\mu_1 + \mu_2)(\mu_1 \lambda/\Delta E(1,4) - \mu_2 \lambda/\Delta E(2,3))}{(E(\mu \mathrm{E}_1) - 2\hbar\omega)\,\Delta E} \tag{135}$$

$$\text{(b)} \qquad \epsilon_0 \chi^{(2)}_{xxx} = \mathrm{i}\frac{3}{2}c^2 \frac{\bar{v}_z}{\Delta E_z} \bar{p} q \langle S_y \rangle \sum_{\mu} \frac{(\mu_1 + \mu_2)(\mu_1 \lambda/\Delta E(1,3) - \mu_2 \lambda/\Delta E(2,4))}{(E(\mu \mathrm{E}_1) - 2\hbar\omega)\,\Delta E}. \tag{136}$$

The results obtained here combined together—that is, $\chi_{\alpha\alpha\alpha} = \chi^{(1)}_{\alpha\alpha\alpha} + \chi^{(2)}_{\alpha\alpha\alpha}$—will be compared with observation [16] in the next section.

The expressions for the i-tensors, χ_{zxx} and χ_{zzz}, in the exciton mode can be obtained simply by replacing E_1 in the denominators of equations (80) and (83) by the exciton energy $E(\mathrm{A}_1)$ obtained in section 5.2. The result for χ_{xxz} in the exciton mode is given by

$$\chi_{xxz} = 3 \sum_{\mu} \frac{((P_x)_{01}\mu_1 + (P_y)_{02}\mu_2)((P_x P_z)_{10}\mu_1 + (P_y P_z)_{20}\mu_2)}{(E(\mu \mathrm{E}_1) - 2\hbar\omega)\,\Delta E}. \tag{137}$$

The matrix elements appearing in this equation are the same as those in equation (85).

We have obtained the susceptibilities $\chi^{(c)}$ in forms proportional to the magnetization $\langle S_x \rangle$ or $\langle S_y \rangle$ of the Mn_1 sublattice and regarded, e.g., $\langle S_x \rangle$ as an order parameter in case (a). According to Birss [12], however, the order parameter in case (a) should be the yyy-component of a third-rank tensor and made up of a complicated combination of spin components of the six Mn ions in the unit cell as given by Nedlin [13] or Sa *et al* [14]. Therefore it will be in order here to make clear the relation between Birss's order parameter and our $\langle S_x \rangle$.

The spin ordering with symmetry (a), i.e., $P6'_3cm'$, is described by the order parameter $\psi_3 = (\sigma_1^- + \sigma_2^+)/2$ in Nedlin's notation. Similarly, the ordering with symmetry (b) $P6'_3c'm$ is described by $\psi_4 = (-\sigma_1^- + \sigma_2^+)/2\mathrm{i}$. Sa *et al* show with the aid of phenomenological theory based on symmetry considerations that $\chi^{(c)}_{yyy}$ in case (a) and χ_{xxx} in case (b) are proportional to the order parameters ψ_3 and ψ_4, respectively. The parameter ψ_3 (ψ_4) behaves like the basis of the irreducible representation B_1 (B_2) of $\mathrm{C}_{6\mathrm{v}}$. In other words, it transforms like $y^3 - 3x^2y$ ($x^3 - 3xy^2$) as shown on the right of table 1, which implies that ψ_3 (ψ_4) is indeed a component of a third-rank tensor.

We have mentioned in the above that ψ_3 and ψ_4 are complicated combination of spin components. The complexity is, however, only superficial. Let us denote, for example, the (local) ξ_i-component of the spin vector $\boldsymbol{S}_i$ of Mn_i by $S_{i\xi}$. Then it is not difficult to show that they may be expressed in terms of $S_{i\xi}$ simply as

$$\psi_3 = \sum_{i=1}^{3} S_{i\xi} - \sum_{i=4}^{6} S_{i\xi} \tag{138}$$

$$\psi_4 = \sum_{i=1}^{3} S_{i\eta} - \sum_{i=4}^{6} S_{i\eta} \tag{139}$$

with our choice of local coordinate systems. In the microscopic theory, we replace the classical quantities $S_{i\xi}$, etc, by the corresponding quantum mechanical thermal averages $\langle S_{i\xi}\rangle$, etc. Recalling that the magnetizations of the six sublattices are given by $\langle S_{i\xi}\rangle = -\langle S_{i+3\,\xi}\rangle = \langle S_x\rangle$ $(i = 1, 2, 3)$ in case (a), we can set $\psi_3 = 6\langle S_x\rangle$. In a similar way, we obtain $\psi_4 = 6\langle S_y\rangle$ in case (b). Finally, it is worth pointing out that we have another order parameter ψ_3' in case (a), which also transforms like B_1 and describes the canting of the spins out of the xy-plane. That is, we have

$$\psi_3' = \sum_{i=1}^{3} S_{iz} - \sum_{i=4}^{6} S_{iz} \tag{140}$$

which is also replaced by $6\langle S_z\rangle$ in quantum theory.

6. Comparison with experiments

6.1. Clamping of order parameters

We have seen in the previous section that, for example, χ_{yyy} consists of two terms proportional either to v_{zx} or to $\bar{v}_z$ besides the sublattice magnetization $\langle S_x\rangle$. In other words, it is bilinear with respect to the two order parameters, electric and magnetic [14], because, in the ferroelectric (fel) phase, the parameters v_{zx} and $\bar{v}_z$ will have different signs in the domains with positive and negative electric polarization, which are denoted as fel+ and fel−, respectively. Note that the environment of the Mn_1 ion in fel+ is carried into that of the corresponding Mn_1' ion in fel− by the operation of σ_h $(z \to -z)$ [6]. The magnetic susceptibility regarded as a function of position will change its sign upon crossing the fel domain boundary even when $\langle S_x\rangle$ does not change its sign. This then implies that, if we only monitor $\chi^{(c)}$, the boundary between fel+ and fel− will be associated (incorrectly) with the boundary of the two neighbouring antiferromagnetic (afm) domains. The brightness change observed in $\chi^{(c)}$ will occur at the same boundary as that in $\chi^{(i)}$. In such cases, we should expect correlations between the observed fel and afm domain boundaries. Apparently, however, the fel and afm structure *do not influence each other*, according to experiments [15]. In order to explain this independence, we have to assume that the spins $\boldsymbol{S}$ are reversed within a few atomic layers when crossing a fel border. Let us denote the magnetic domain with $\boldsymbol{S} \parallel \boldsymbol{x}$ and that with $\boldsymbol{S} \parallel -\boldsymbol{x}$ as afm+ and afm−, respectively. If this happens, the magnetic domain afm+ in fel+, or the combination (++), the first + being for fel and the second + for afm, and afm− in fel−, or (−−), in contact with the former, will be observed as a single domain, EM+, extending over the two fel domains fel+ and fel− which share the boundary.

We summarize our ideas for $P6_3'cm'$ in table 2.

Note that, in the table, EM+, (++), and (−−), are the domains with + brightness, while EM−, (+−), and (−+), are those with − brightness. The *apparent* independence of the fel

Table 2. Clamping of order parameters.

	afm+	afm−	
fel+	EM+ = (++)	EM− = (+−)	$\chi^{(i)}_{zxx} > 0$
fel−	EM− = (−+)	EM+ = (−−)	$\chi^{(i)}_{zxx} < 0$

and afm structure is attributed to the clamping of the afm order with the fel order, as shown in the second and third columns of the table. This is in accord with the idea that the electronic states of the Mn_1 and $Mn_{1'}$ ions, each located near the boundary of the two fel domains in contact, are connected by the operation of σ_h, including the spin as well as the orbital state. We admit that the idea is only an *ad hoc* assumption and that some more physical reason for such a relation is necessary. For example, it would be nice if we could show that the reversal of the spin across the fel domain wall is energetically more favourable. In fact, we have attempted a computer simulation for the spin reversal, and confirmed for the model adopted that EM+ (++) in contact with EM+ (−−) can be lower in energy than EM+ (++) in contact with EM− (−+), if just changes in the values of the exchange integrals of appropriate sign and magnitude are introduced between the magnetic ions *within the walls* between the fel+ and fel− domains. It is not that EM+ (−−) and EM− (−+) have different energies. These two domains can coexist within a single fel− domain. That is to say, EM+ (−) in one fel domain can share the fel domain boundary only with an EM+ (−) domain and not with EM− (+) in the neighbouring fel domain. However, it would be premature to go further into the details of this model calculation, because, at present, we know almost nothing about the possible structural change which would take place within those layers and bring about such a change of coupling parameters for the coupling between the spins.

Anyway, we do not think, *within the framework of the present theory,* that any other interpretation is possible for the observed apparent independent behaviours of the two structures, unless we assume this kind of clamping of order parameters.

6.2. Calculated and observed SHG spectra

We have derived the microscopic expressions for χ_{yyy} for case (a) and χ_{xxx} for case (b), and χ_{zxx} for both cases in the previous section. In this section, we will calculate the spectra for these susceptibilities numerically and compare them with the observed ones.

We introduce here the relaxation effects so as to satisfy causality, and express the susceptibilities for both cases from equations (133) to (136) as follows:

(a)
$$\begin{aligned}\chi^{(1)}_{yyy} + \chi^{(2)}_{yyy} &\propto -\mathrm{i}\Bigg[\sum_{\nu} \frac{(\nu_1/\Delta E(1,4) - \nu_2/\Delta E(2,3))(\nu_1/\Delta E(1,3) - \nu_2/\Delta E(2,4))}{E(\nu \mathrm{E}_2) - 2\hbar\omega - \mathrm{i}\Gamma(\nu \mathrm{E}_2)} \\ &\quad + \sum_{\mu} \frac{(\mu_1/\Delta E(1,3) - \mu_2/\Delta E(2,4))(\mu_1/\Delta E(1,4) - \mu_2/\Delta E(2,3))}{E(\mu \mathrm{E}_1) - 2\hbar\omega - \mathrm{i}\Gamma(\mu \mathrm{E}_1)}\Bigg] \\ &\quad + \mathrm{i}r \sum_{\mu} \frac{(\mu_1/\Delta E(1,3) + \mu_2/\Delta E(1,3))(\mu_1/\Delta E(1,4) - \mu_2/\Delta E(2,3))}{E(\mu \mathrm{E}_1) - 2\hbar\omega - \mathrm{i}\Gamma(\mu \mathrm{E}_1)}\end{aligned} \tag{141}$$

(b)
$$\begin{aligned}\chi^{(1)}_{xxx} + \chi^{(2)}_{xxx} &\propto \mathrm{i}\Bigg[\sum_{\nu} \frac{(\nu_1/\Delta E(1,3) - \nu_2/\Delta E(2,4))^2}{E(\nu \mathrm{E}_2) - 2\hbar\omega - \mathrm{i}\Gamma(\nu \mathrm{E}_2)} \\ &\quad - \sum_{\mu} \frac{(\mu_1/\Delta E(1,3) - \mu_2/\Delta E(2,4))^2}{E(\mu \mathrm{E}_1) - 2\hbar\omega - \mathrm{i}\Gamma(\mu \mathrm{E}_1)}\Bigg] \\ &\quad + \mathrm{i}r \sum_{\mu} \frac{(\mu_1/\Delta E(1,3) + \mu_2/\Delta E(1,3))(\mu_1/\Delta E(1,3) - \mu_2/\Delta E(2,4))}{E(\mu \mathrm{E}_1) - 2\hbar\omega - \mathrm{i}\Gamma(\mu \mathrm{E}_1)}\end{aligned} \tag{142}$$

where

$$r = \frac{1}{cc'}\left(\frac{\bar{v}_z}{v_{zx}}\right)\left(\frac{\bar{p}}{p}\right)\frac{\Delta E(1,3)}{\Delta E_z}. \tag{143}$$

Note that $E(\nu\mathrm{E}_2)$ and $E(\mu\mathrm{E}_1)$ are the eigenvalues of the matrices (117) and (119), respectively. Therefore, given parameters E_i $(i = 1, 2, 3, 4)$, K_i, K_i', $\overline{K}_i$ $(i = 1, 2)$, K, $\overline{K}$, four Γs, and r, we can readily obtain the SHG spectra from the above equations.

The observation of $\chi^{(i)} \equiv \chi_{zxx}$ gives the position of the excited level at 2.7 eV in all of the systems [2]. The condition

$$E(\mathrm{A}_1) = E_1 - 2K_1 - K_1' + 2\overline{K}_1 = 2.7\ \mathrm{eV} \tag{144}$$

which follows from equation (115) must be satisfied, because χ_{zxx} is given by replacing E_1 in the denominator of equation (80) by $E(\mathrm{A}_1)$ of the present equation. Here and hereafter we will neglect K_i' and $\overline{K}_i$ $(i = 1, 2)$ which are inter-layer transfer-matrix elements compared to the intra-layer ones K_1 and K_2. Then the splitting of 0.05 eV at around 2.45 eV is estimated from the perturbational calculation as

$$E(\mu = -, \mathrm{E}_1) - E(\nu = -, \mathrm{E}_2) = \frac{36K\overline{K}}{E_1 + K_1 - E_2 - K_2}. \tag{145}$$

Five energy parameters, E_1, K_1, E_2, K, and $\overline{K}$, have been fixed as shown in table 3 from these two equations (144) and (145) and the observed three lowest energies as mentioned at the end of section 5.2. The parameter K_2 is set to zero. Three other material constants, E_3, E_4, and r, are estimated from the relative magnitudes of the SHG at the second, third, and fourth peaks to that of the first at 2.46 eV. Incidentally, the value chosen for the energy $E_4 = 1.57$eV nearly agrees with the location of the absorption edge observed at 1.55 eV [1]. The relaxation constants are determined so as to reproduce the SHG spectra obtained through the observations under the specified condition of polarization.

Table 3. The material constants: $E_i (i = 1, 2, 3, 4)$, K_1, K, $\overline{K}$ in eV, which are used in the numerical calculation of SHG spectra in each case of figure 2.

	E_1	E_2	E_3	E_4	K_1	K	$\overline{K}$
(a) $YMnO_3$	2.68	2.55	2.1	1.57	−0.01	0.037	−0.011
(a′) $HoMnO_3$ ($T = 6$ K)	2.68	2.57	2.1	1.57	−0.01	0.045	−0.014
(b) $ErMnO_3$	2.68	2.57	2.15	1.57	−0.01	0.045	−0.014
(b′) $HoMnO_3$ ($T = 50$ K)	2.68	2.57	2.1	1.57	−0.01	0.045	−0.014

Table 4. The material constants: r and the Γs in eV, which are used in the numerical calculation of the SHG spectra for each case of figure 2.

	r	$\Gamma(-, \mathrm{E}_2)$	$\Gamma(-, \mathrm{E}_1)$	$\Gamma(+, \mathrm{E}_1)$	$\Gamma(+, \mathrm{E}_2)$
(a) $YMnO_3$	0	0.027	0.048	0.18	0.18
(a′) $HoMnO_3$ ($T = 6$ K)	0	0.035	0.05	0.3	0.3
(b) $ErMnO_3$	−5.3	0.03	0.03	0.17	0.17
(b′) $HoMnO_3$ ($T = 50$ K)	−5.8	0.028	0.028	0.16	0.16

Figure 2 shows the SHG spectra associated with the non-linear susceptibilities $\chi^{(c)}$ of (a) $YMnO_3$, (b) $ErMnO_3$, (a′) $HoMnO_3$ ($T = 6$ K), and (b′) $HoMnO_3$ ($T = 50$ K). Cases (a) and (a′) correspond to χ_{yyy}, and cases (b) and (b′) to χ_{xxx}. In the figure, dots show the experimental data and lines correspond to the numerical data.

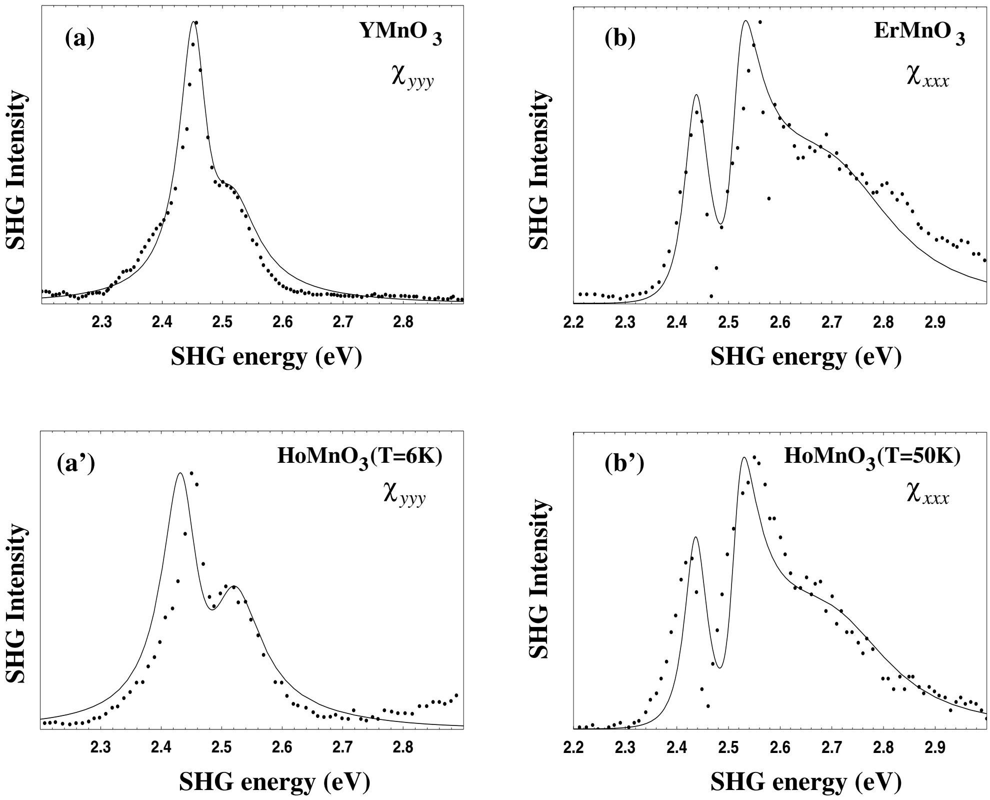

Figure 2. The SHG spectra associated with the non-linear magnetic susceptibilities of (a) $YMnO_3$, (b) $ErMnO_3$, (a′) $HoMnO_3$ ($T = 6$ K), and (b′) $HoMnO_3$ ($T = 50$ K). Dots show the experimental results and lines the numerical ones. The material constants have been fixed as shown in tables 3 and 4.

Now we can understand microscopically the observed SHG spectra of both cases (a) and (b) as follows. First, the two lowest levels by which the SHG is enhanced by two-photon resonance consist of $E(\nu = -, \mathrm{E}_2) = 2.45$ eV and $E(\mu = -, \mathrm{E}_1) = 2.51$ eV for both (a) $YMnO_3$ and (b) $ErMnO_3$. These two signals, however, interfere constructively in case (a) and destructively in case (b). This difference originates from the different relative magnitudes r $(\propto \bar{v}_z/v_{zx})$ of the second to the first term in equations (141) and (142), which correspond, respectively, to cases (a) and (b). We have chosen $r = 0$ for case (a) and $r = -5.3$ for case (b). Second, two higher levels, $E(\mu = +, \mathrm{E}_1)$ and $E(\nu = +, \mathrm{E}_2)$, located at around 2.7 eV are observed with much stronger intensity but larger relaxation in the SHG spectra of case (b), while the SHG signals are almost negligible in case (a) as shown in figure 2(a) and figure 2(a′). This is also due to the different values of r in cases (a) and (b).

The same description applies to the cases of the low-temperature phase (6 K) and the high-temperature phase (50 K) of $HoMnO_3$, respectively, as shown in figure 2(a′) and figure 2(b′).

Two minor deviations remain between the observed and calculated SHG spectra: the observed weak shoulders on the lower-energy side below 2.4 eV and the observed sharper dip due to the destructive interference in figure 2(b) and figure 2(b′). In spite of these two minor deviations, we have succeeded in understanding the following important observations:

(1) Only χ_{yyy} is finite in a form linearly proportional to a product of the sublattice magnetization $\langle S_x \rangle$ and ferroelectric order v_{zx} or $\bar{v}_z$ for cases (a) $YMnO_3$ and (a′) $HoMnO_3$ ($T < 42$ K), while only χ_{xxx} is finite in proportion to $\langle S_y \rangle$ and v_{zx} (or $\bar{v}_z$) for cases (b) $ErMnO_3$ and (b′) $HoMnO_3$ (42 K $< T <$ 71 K) under two-photon resonant excitation around 2.5 eV.

(2) The two SHG signals at 2.45 eV and 2.51 eV interfere constructively for cases (a) and (a′) while they interfere destructively for cases (b) and (b′).

(3) Further, if we assume that the factors omitted in equations (141) and (142) are of the same order of magnitudes and compare the intensity of the spectra in figures 2(a) and 2(a′) to those in figures 2(b) and 2(b′), we find that the former intensities are stronger than the latter ones, although we have given them in arbitrary units in figure 2. This seems to be the case for the observation [3].

(4) Finally, the SHG signals at around 2.7 eV are almost negligible in cases (a) and (a′), while they become of the same order of magnitude as those at the lower energies at 2.45 eV and 2.51 eV for cases (b) and (b′).

7. Discussion and conclusions

As mentioned in section 1, the SHG spectra of $RMnO_3$ pose several interesting problems. First of all, there is the problem of the electronic structure of the Mn ions in this crystal. The Mn^{3+} ions are surrounded by an unusual coordination of five O^{2-} ions. We have assumed an ordering of the energy levels that is almost the same as that proposed in reference [1]. The results obtained in this paper seem to support the assumption. Next, we encounter the appearance of non-vanishing susceptibilities $\chi^{(c)}$ in the antiferromagnetic phase. If we only watch the Mn and their spins, the Mn sublattice in this phase has inversion symmetry (as long as we neglect the canting of spins in the $P6_3'cm'$ phase) and it seems that there will be no SHG. However, it is, of course, not correct to confine our attention just to the Mn sublattice. We have to take into account the full crystal symmetry, where there is no inversion centre in the ferroelectric phase. We have indeed found that non-vanishing $\chi^{(i)}$ as well as $\chi^{(c)}$ resulted from the presence of the low-symmetry fields $V(E_1a) \propto zx$ and $V(B_2) \propto z$ around Mn_1 ions. The appearance of these fields corresponds to the loss of the centre of inversion in the ferroelectric phase. The latter susceptibilities $\chi^{(c)}$ were found to be proportional to the sublattice magnetizations in the present treatment. Our results show that the lower-symmetry case of $P6_3'$ can be derived by a combination of cases (a) and (b), (a) describing the $\langle S_x \rangle$ component and (b) the $\langle S_y \rangle$ component. The two cases do not mix—that is, spin x- and y-components are decoupled. We can predict this independent behaviour of the spin components and it has, in fact, been confirmed by a recent experiment [5]. This brings in the third problem, i.e., the apparent independent behaviours of fel and afm structures observed and discussed in section 6.1. Although we have proposed a possible interpretation, i.e., the clamping of two order parameters, the problem still remains a topic to be investigated further. The fourth is the two peaks of the SHG spectra found in the region of 2.45 eV. As shown in sections 5 and 6, the exciton theory appears to provide us with a reasonable explanation.

The sublattice magnetizations $\langle S_x \rangle$ and $\langle S_y \rangle$ of the Mn_1 ion are correlated with the crystalline structure change of $HoMnO_3$ at 42 K as well as the difference between $YMnO_3$ and $ErMnO_3$. Our understanding is that this difference may be attributed to the relative magnitude of the lower-symmetry crystalline fields $V(B_2)$ and $V(E_1a)$ which act on Mn ions in the electronic ground state. This is because the spectroscopic difference in SHG between cases (a), $P6_3'cm'$, and (b), $P6_3'c'm$, originates from the different relative magnitudes of $\bar{v}_z/v_{zx}$ as indicated by the values of r.

The third problem, the clamping of the ferroelectric and antiferromagnetic order parameters, should be verified by the following experiments now in preparation[2].

(1) If the model is correct, we should observe reversal of brightness or contrast of the SHG signal in (a) $YMnO_3$, i.e., EM$\pm \to$ EM$\mp$, while the contrast will not change in (b) $ErMnO_3$, EM$\pm \to$ EM$\pm$, when thin samples are rotated by π around the x-axis. In these experiments, an external reference is involved which leads to differing brightness due to the differing interference for different domains.

(2) When the samples are rotated around the y-axis, we expect reversal of contrast in $ErMnO_3$, but not in $YMnO_3$. If there is no clamping, opposite behaviours of the contrast would be observed, and this would allow us to reject the possibility of a bilinear dependence of χ on the two order parameters.

While the present paper was in preparation, the work by Wan *et al* [17] appeared. These authors also deal with the non-linear susceptibilities χ_{xxx}, etc, for $YMnO_3$, within the multi-band Hubbard model, taking into account the charge transfer between O^{2-} and Mn^{3+} in addition to the d–d transitions. They, however, assume perovskite instead of hexagonal structure, besides neglecting the spin–orbit interaction which is essential in our treatment for producing the susceptibility tensors $\chi^{(c)}$ with correct selection rules, so it is not conceivable that their theory will be able to explain the observation, i.e., non-vanishing $\chi^{(c)}_{yyy}$ in $P6_3'cm'$ ($YMnO_3$) and $\chi^{(c)}_{xxx}$ in $P6_3'c'm$ ($ErMnO_3$).

Acknowledgments

The authors have benefited considerably from discussion with M Fiebig and R V Pisarev. They especially thank M Fiebig for informing them of experimental findings prior to publication and reviewing the present paper critically during the course of its preparation.

Appendix A. The mechanism of exciton transfer

In order to discuss the excitation transfer between Mn ions, we first give the Slater determinants for the electronic states given in section 3, expressed in terms of the one-electron orbitals φ_{zx}, etc:

$$\Phi_{zx} = +|\varphi_{zy}, \varphi_{x^2-y^2}, \varphi_{-2xy}, \varphi_{z^2}| \tag{A.1}$$

$$\Phi_{zy} = -|\varphi_{zx}, \varphi_{x^2-y^2}, \varphi_{-2xy}, \varphi_{z^2}| \tag{A.2}$$

$$\Phi_{x^2-y^2} = +|\varphi_{zx}, \varphi_{zy}, \varphi_{-2xy}, \varphi_{z^2}| \tag{A.3}$$

$$\Phi_{-2xy} = -|\varphi_{zx}, \varphi_{zy}, \varphi_{x^2-y^2}, \varphi_{z^2}| \tag{A.4}$$

$$\Phi_{z^2} = +|\varphi_{zx}, \varphi_{zy}, \varphi_{x^2-y^2}, \varphi_{-2xy}| \tag{A.5}$$

where spins are assumed to be quantized along appropriate local axes. The matrix elements of the angular momenta connecting the ground and excited states are easily found as

$$\langle\Phi_{zx}|L_y|\Phi_{z^2}\rangle = -\langle z^2|\ell_y|zx\rangle = +\mathrm{i}\sqrt{3} \tag{A.6}$$

$$\langle\Phi_{zy}|L_x|\Phi_{z^2}\rangle = -\langle z^2|\ell_x|zy\rangle = -\mathrm{i}\sqrt{3}. \tag{A.7}$$

Let us denote the integral for transfer between orbitals 1 and 2 by $t(1, 2)$. The result of the second-order perturbation corresponding to the excitation transfer between Mn_1 (excited,

[2] This idea is due to M Fiebig and the experiments are going to be carried out at Dortmund.

site 01) and Mn_2 (de-excited, site $n2$) shown in figure A1 leads to the following expression for the interaction term in the Hamiltonian:

$$\mathcal{H}'_{12} = -\sum_{\sigma,\sigma'} \frac{t(2',1')t(1,2)}{\Delta E(1 \leftarrow 2)} \xi^\dagger_{2'\sigma'}\xi_{1'\sigma'}\xi^\dagger_{1\sigma}\xi_{2\sigma} - \sum_{\sigma,\sigma'} \frac{t(1,2)t(2',1')}{\Delta E(2' \leftarrow 1')} \xi^\dagger_{1\sigma}\xi_{2\sigma}\xi^\dagger_{2'\sigma'}\xi_{1'\sigma'} \tag{A.8}$$

in the second-quantized form, where $\xi^\dagger_{1\sigma}$ and $\xi_{1\sigma}$ are, respectively, the creation and annihilation operators for the electron in the orbital 1 with spin σ.

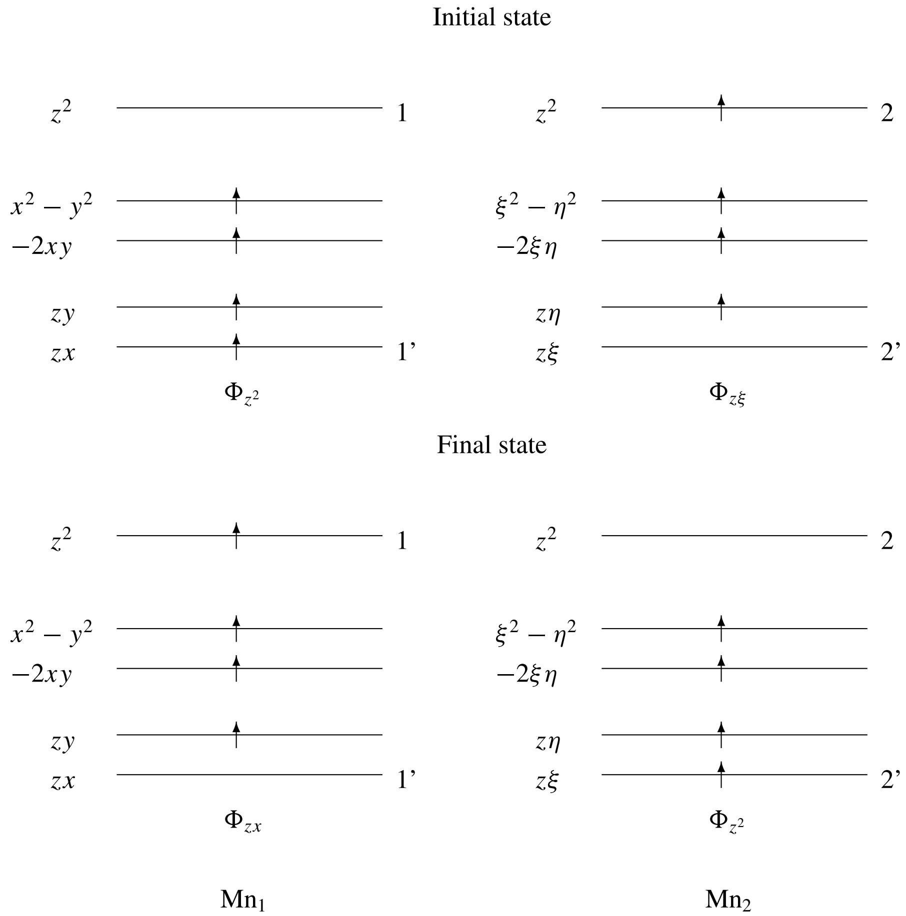

Figure A1. Excitation transfer between ions Mn_1 and Mn_2.

The right-hand side of this equation may be rewritten as

$$\mathcal{H}'_{12} = k(12', 1'2)\left(\frac{1}{2}\hat{n}_{11'}\hat{n}_{2'2} + 2\boldsymbol{s}_1\hat{n}_{11'} \cdot \boldsymbol{s}_2\hat{n}_{2'2}\right) \tag{A.9}$$

where

$$k(12', 1'2) = \frac{t(2',1')t(1,2)}{\Delta E(1 \leftarrow 2)} + \frac{t(1,2)t(2',1')}{\Delta E(2' \leftarrow 1')} \tag{A.10}$$

with

$$\hat{n}_{11'} = \sum_\sigma \xi^\dagger_{1\sigma}\xi_{1'\sigma} \tag{A.11}$$

and

$$s_1\hat{n}_{11'} = \sum_{\sigma,\sigma'} \langle\sigma|s|\sigma'\rangle \xi^{\dagger}_{1\sigma}\xi_{1'\sigma'}. \tag{A.12}$$

If we set

$$|1'\rangle = \varphi_{zx}(01) \qquad |1\rangle = \varphi_{z^2}(01) \tag{A.13}$$

$$|2'\rangle = \varphi_{z\xi}(n2) \qquad |2\rangle = \varphi_{z^2}(n2) \tag{A.14}$$

we find

$$\hat{n}_{11'} = \sum_{\sigma} \langle z^2|\ell_y|zx\rangle \xi^{\dagger}_{1\sigma}\xi_{1'\sigma}/(-\mathrm{i}\sqrt{3}) \tag{A.15}$$

$$\hat{n}_{2'2} = \sum_{\sigma} \langle z\xi|\ell_\eta|z^2\rangle \xi^{\dagger}_{2'\sigma}\xi_{2\sigma}/(+\mathrm{i}\sqrt{3}) \tag{A.16}$$

so we obtain

$$W_{01,n2} = k_{x\xi}w(1y,2\eta) + k_{y\eta}w(1x,2\xi) - k_{x\eta}w(1y,2\xi) - k_{y\xi}w(1x,2\eta) \tag{A.17}$$

for the expression for $W_{01,n2}$ in equation (98) of section 5.2, where, for example,

$$w(1y,2\eta) = \frac{1}{3}\left\{\frac{1}{2}\ell_{1y}\ell_{2\eta} + 2s_1\ell_{1y}\cdot s_2\ell_{2\eta}\right\} \tag{A.18}$$

and $k_{x\xi} \equiv k_{x\xi}(01, n2)$, etc, are defined by

$$k_{x\xi} = k(01zx\ n2z^2, 01z^2\ n2z\xi) \qquad k_{y\eta} = k(01zy\ n2z^2, 01z^2\ n2z\eta) \tag{A.19}$$

$$k_{x\eta} = k(01zx\ n2z^2, 01z^2\ n2z\eta) \qquad k_{y\xi} = k(01zy\ n2z^2, 01z^2\ n2z\xi). \tag{A.20}$$

Note that we may set

$$w(1y,2\eta) = \frac{1}{3}F_{12}L_y(01)L_\eta(n2) \tag{A.21}$$

in terms of the components of the total orbital angular momenta with

$$F_{12} = \frac{1}{2} + 2S_1\cdot S_2/16 \tag{A.22}$$

in equation (A.18), because $s = S/4$. Note that $F_{12} = F_{15} = 1/4$, $F_{14} = 1$ in the classical approximation.

References

[1] Fröhlich D, Leute St, Pavlov V V and Pisarev R V 1998 *Phys. Rev. Lett.* **81** 3239
Note that we refer in the text to the data given in this and the next reference as corrected by reference [3]. To denote antiunitary operators, primes instead of underlines have been used in the present paper.

[2] Fröhlich D, Leute St, Pavlov V V, Pisarev R V and Kohn K 1999 *J. Appl. Phys.* **85** 4762

[3] Fiebig M, Fröhlich D, Kohn K, Leute St, Lottermoser Th, Pavlov V V and Pisarev R V 2000 *Phys. Rev. Lett.* **84** 5620
The choices of x- and y-axes, and the selection rules employed in the previous reports [1, 2] are revised in this letter.

[4] Yakel K L, Koehler W C, Bertaut E F and Forrat E F 1963 *Acta Crystallogr.* **16** 27

[5] Fiebig M, Fröhlich D, Lottermoser Th and Kohn K 2000 *Appl. Phys. Lett.* **77** 4401

[6] Iliev M N, Lee H-G, Popov V N, Abrashev M N, Hamed A, Meng R L and Chu C W *Phys. Rev.* **56** 2488

[7] Inui T, Tanabe Y and Onodera Y 1996 *Group Theory and Its Applications in Physics* (Berlin: Springer)
Note that, in the character table for D_{3h} of this book (table B.8 on p 387), the twofold axis is chosen as the y-axis, in contrast to the choice in the present paper.

[8] Muthukumar V N, Valenti R and Gros C 1995 *Phys. Rev. Lett.* **75** 2786
Muthukumar V N, Valenti R and Gros C 1995 *Phys. Rev.* B **54** 433

[9] Muto M, Tanabe Y, Iizuka-Sakano T and Hanamura E 1998 *Phys. Rev.* B **57** 9586
[10] Tanabe Y, Muto M, Fiebig M and Hanamura E 1998 *Phys. Rev.* B **58** 8654
[11] Allen J W, Macfarlane R M and White R L 1969 *Phys. Rev.* **179** 523
[12] Birss R R 1966 *Symmetry and Magnetism* (Amsterdam: North-Holland)
[13] Nedlin G M 1965 *Sov. Phys.–Solid State* **6** 2156
[14] Sa D, Valenti R and Gros C 2000 *Eur. Phys. J.* B **14** 301
[15] Fiebig M 2000 private communication
[16] Fiebig M, Fröhlich D, Leute St, Lottermoser Th, Pavlov V V and Pisarev R V 2001 *J. Magn. Magn. Mater.* at press
[17] Wan X, Dong J, Qian M and Zhang W 2000 *Phys. Rev.* B **61** 10 664